

ABSTRACT

Polycyclic Aromatic Hydrocarbon Absorption and Permeability of Firefighter Hoods

Ryan Deitz

Director: Debra Harris, Ph.D.

Firefighters face more dangers than fire and smoke. Their equipment is designed to protect them from the immediate operational hazards, but many firefighters will develop chronic illnesses such as cancer. Exposure to toxic chemical substances originating from fires affects the lives of firefighters internationally every year. One common group of potential carcinogens present in fire is polycyclic aromatic hydrocarbons (PAH). Studies regarding PAH contamination in firefighters after missions highlight the neck as a potential hotspot for dermal absorption. In firefighter gear, the hood is the component which best protects the neck. This thesis scrutinizes a standard Ara-Tek FR™ Tri-Blend Hood's ability to absorb PAHs from smoke by filtering smoke simultaneously through a hood filter and a control hoodless filter. To collect contaminants, smoke was bubbled into water and subsequently extracted through solid phase extraction (SPE) cartridges. Gas Chromatography-Mass Spectrometry (GCMS) was used to separate and identify sample compounds. None of the chromatogram peaks in the control and filtered samples matched those in the PAH standard, however other chemicals of concern were identified. This preliminary experiment provided data that suggests further research on materials and methods for evaluating firefighter hood effectiveness to block chemical contaminants.

APPROVED BY DIRECTOR OF HONORS THESIS:

A handwritten signature in black ink, appearing to read 'D. Harris', written over a horizontal line.

Dr. Debra Harris, PHD, Human Sciences and Design

APPROVED BY HONORS PROGRAM:

A solid horizontal line intended for a signature.

Dr. Andrew Wisely, Interim Director

DATE: _____

POLYCYCLIC AROMATIC HYDROCARBON ABSORPTION AND
PERMEABILITY IN FIREFIGHTER HOODS

A Thesis Submitted to the Faculty of
Baylor University
In Partial Fulfillment of the Requirements for the
Honors Program

By
Ryan Deitz

Waco, Texas

May 2021

TABLE OF CONTENTS

List of Figures	iii
List of Tables	v
Acknowledgments	vi
Chapter One: Introduction	1
Chapter Two: Review of Literature	3
Potential Exposure to PAH Particles	3
Firefighter Hoods	5
Chapter Three: Methodology.	7
Filtration Experiment.	7
GC-MS Analysis	10
Chapter Four: Results.	11
Chapter Five: Discussion	15
Experimental Limitations and Areas for Improvement.	16
Carbon Nanomaterial Hoods.	18
Chapter Six: Conclusion	19
Appendices	20
Appendix A: PAH Standard Mix	21
Appendix B: Table 1 Identification	30
Bibliography	53

LIST OF FIGURES

Figure 1. Smoking Rig Prior to Testing	8
Figure 2. Smoke Filtration in Progress.	9
Figure 3. Side-by-Side Comparison of Sample Chromatograms	11
Figure 4. Chromatogram of PAH Standard Mix	12
Figure A.1. Naphthalene	21
Figure A.2. Acenaphthylene.	22
Figure A.3. Acenaphthene	22
Figure A.4. Fluorene	23
Figure A.5. Acenaphthylene, 1-bromo.	23
Figure A.6. Phenanthrene	24
Figure A.7. Anthracene.	24
Figure A.8. Carbazole	25
Figure A.9. 9,10-Anthracenedione	25
Figure A.10. Fluoranthene	26
Figure A.11. Pyrene	26
Figure A.12. Benz[a]anthracene	27
Figure A.13. Benz[e]acephenanthrylene	27
Figure A.14. Indole[1,2,3-cd]pyrene at 28.86 Minutes	28
Figure A.15. Benzo[b]triphenylene	28
Figure A.16. Indole[1,2,3-cd]pyrene at 29.40 Minutes	29
Figure B.1. Nonane	30
Figure B.2. Benzene, 1-ethyl-3-methyl-	31

Figure B.3. Cyclotetrasiloxane, octamethyl-	31
Figure B.4. Benzene, 1,2,4-trimethyl-	32
Figure B.5. 1-Hexanol, 2-ethyl	32
Figure B.6. Undecane	33
Figure B.7. Cyclopentasiloxane, decamethyl-	33
Figure B.8. 1H-indene, 1-methylene-	34
Figure B.9. Dodecane	34
Figure B.10. Benzeneethanamine, 2,5-dimethoxy-a-methyl	35
Figure B.11. 3,5-Dimethoxytoluene	35
Figure B.12. Phenol, 4-ethyl-2-methoxyl-	36
Figure B.13. Cyclohexasiloxane, dodecamethyl-	36
Figure B.14. Benzocycloheptatriene	37
Figure B.15. 2-Methoxy-4-vinylphenol	37
Figure B.16. 2(3H)-Furanone, 5-butyldihydro-4-methyl, cis-	38
Figure B.17. Benzaldehyde, 2,3-dimethoxy-	38
Figure B.18. 3-Allyl-6-methoxyphenl	39
Figure B.19. Phenol, 2-methoxy-4-propyl	39
Figure B.20. Benzene, 1,2,3-trimethoxy-5-methyl-	40
Figure B.21. Phenol, 2-methoxy-4-(1-propenyl)- at 12.85 Minutes	40
Figure B.22. 2,5-Dimethoxybenzyl alcohol	41
Figure B.23. Phenol, 2-methoxy-4-(1-propenyl)- at 13.43 Minutes	41
Figure B.24. Cycloheptasiloxane, tetradecamethyl-	42
Figure B.25. 5-tert-Butylpyrogallol	42

Figure B.26. 2,5-Dimethoxybenzyl alcohol	43
Figure B.27. Pentanoic acid, 2,2,4-trimethyl-3carboxyisopropyl ester	43
Figure B.28. Phenol, 2,6-dimethoxy-4-(2-propenyl)- at 15.20 Minutes	44
Figure B.29. 2,4-Hexadienic acid, 3,4-diethyl-, dimethyl ester	44
Figure B.30. Cyclooctasiloxane, hexadecamethyl-	45
Figure B.31. Phenol, 2,6-dimethoxy-4-(2-propenyl)- at 15.80 Minutes	45
Figure B.32. Phenol, 2,6-dimethoxy-4-(2-propenyl)- at 16.39 Minutes	46
Figure B.33. Cyclonasiloxane, octadecamethyl- at 17.30 Minutes	46
Figure B.34. 2,3-Dimethoxy-5-aminocinnamitrile	47
Figure B.35. Butyl citrate	47
Figure B.36. Cyclonasiloxane, octadecamethyl- at 18.81 Minutes	48
Figure B.37. 1H,15H-hexadecamethyloctasiloxane	48
Figure B.38. Hexadecanoic acid, butyl ester	49
Figure B.39. Cyclonasiloxane, octadecamethyl- at 21.43 Minutes	49
Figure B.40. Cyclonasiloxane, octadecamethyl- at 22.59 Minutes	50
Figure B.41. Cyclonasiloxane, octadecamethyl- at 23.68 Minutes	50
Figure B.42. Phthalic acid, di(oct-3-yl) ester	51
Figure B.43. Cyclonasiloxane, octadecamethyl- at 24.72 Minutes	51
Figure B.44. 1,4-Benzenedicarboxylic acid, bis(2-ethylhexyl) ester	52

LIST OF TABLES

Table 1. Sample Peak Identification Table with Select Probabilities	13
---	----

ACKNOWLEDGMENTS

I would like to thank my advisor and benefactor of this thesis Dr. Debra Harris, without whom this project would have never come to fruition. She has worked tirelessly to guide my efforts towards meaningful ends. Thank you offering your expertise, time, and energy. You have helped convince me that my time has not been wasted.

I would also like to thank Drew Stolpman for offering his assistance when we were in dire need of it. You were instrumental in allowing us to kickstart this project, and your efforts are deeply appreciated.

Of course, I need to offer my most heartfelt gratitude to Dr. Klaudia Kocurek of Texas A&M for lending her mass spectrometer to our cause and for greatly assisting in the analysis of our samples. You stepped in to help us exactly when we needed it and you deserve a place of high esteem as may be awarded from this thesis.

Finally, I would like to thank my committee for their review and sage comments intended to improve this effort. Thank you for offering your time and expertise, as it allows me to improve as I ought to.

CHAPTER ONE

Introduction

Firefighters are regularly subject to exposure from toxic chemical substances during structure fire events. Despite the abilities of protective gear to safeguard firefighters from burn damage and smoke inhalation, many still succumb to firefighting-related cancers. Jeong et al. (2018) identified significant changes away from normal expression for 9 micro RNAs in 52 incumbent firefighters, with decreased expression of 6 tumor-suppressing miRNAs and increase in 2 potentially cancer-inducing miRNAs. Many of the harmful gaseous agents which firefighters regularly encounter are polycyclic aromatic hydrocarbons (PAHs). The National Institutes of Health identifies the dangers of PAH exposure as respiratory irritation and potential carcinogenesis. They are often released with the combustion of coal, trash, tobacco, gasoline, and wood (2017). There are many molecules which fit the descriptors of polycyclic aromatic hydrocarbons, but the Environmental Protection Agency notes seven as potentially carcinogenic: benzo[a]pyrene, benz[a]anthracene, benzo[b]fluoranthene, benzo[k]fluoranthene, chrysene, dibenz[a,h]anthracene, and indeno[1,2,3-cd]pyrene (2017). Encountering these and several other dangerous airborne compounds is a common occupational hazard for firefighters. The primary goal of this thesis is to determine how effectively a piece of firefighting gear, namely the hood, can filter PAHs and protect the wearer.

Monitoring PAH contamination despite the compound group's ubiquity in the natural environment is crucial due to the observed dangers associated with PAH exposure. In 1998, Topinka et al. demonstrated the mutating effect of PAHs towards rat

cells. Cells demonstrated substantial levels of adduction with the PAH compounds, especially if the PAHs were nitro-PAHs. The complexity of these molecules allows them to participate in a wide variety of interactions with biomolecules. Noted by Yu 2002 as well as many others is the dangerous tendency for interactions between DNA and PAHs. As DNA serves to direct the production of cell proteins, long term exposure allows for PAH-induced mutations of DNA which may result in catastrophic consequences for an organism, such as carcinogenesis. Yu identifies three common pathways for DNA-PAH interaction as diolepoxide formation, free radical intermediates, and nitro reduction. He further specifies that the aromatic nature of Polycyclic Aromatic Hydrocarbons means that they can absorb light in the UV and Visible regions. Comparing in-cell PAH toxicity in the presence and absence of light reveals that the compounds may be over 100 times more toxic when absorbing light (2002).

The personal protective equipment firefighters wear shields firefighters from burns but may allow a considerable amount of volatile toxins to pass through to the skin. The most common pathway to PAH absorption in firefighters which researchers look towards is dermal. The region of particular interest in this thesis is the neck, as according Fent et al. (2014) this area would receive the most contamination after fires. The portion of standard firefighter PPE that covers the neck is the hood. It is likely that most PAHs which reach the neck through the hood are carried by smoke. To test the efficacy of hoods as smoke filters, we modified an experiment performed by Parker et al. (2018). By measuring the PAHs in smokey water compared to smokey water filtered through a firefighter's hood material, we may better understand the current effectiveness of the standard equipment used today.

CHAPTER TWO

Review of Literature

Potential Exposure to PAH Particles

When determining a firefighter's exposure to PAHs, the neck is a common area of interest. As noted by Fent et al. (2014), a firefighter's neck often shows the greatest increase in PAH concentration after controlled structure burns, observing a post-fire median contamination of $52.0 \mu\text{g m}^{-2}$ after the initial round of testing and a median of $62.9 \mu\text{g m}^{-2}$ after the second. Fent et al. propose that the Nomex[®] hoods used in their study may be too chemically permeable. This literature review will discuss the level of exposure firefighters experience with PAHs and how effective current hoods are at protecting from dermal absorption. To this end, we will discern the concentration of PAHs found in water after smoke has been passed through a control pathway and a pathway filtered with a hood fabric sample.

To determine the efficacy of hoods against PAHs, both the quantity of PAHs found on the hoods and the PAHs present in the air during a fire must be measured. Blomqvist et al. (2012) conducted multiple burn tests with flame retarded (FR) and non-altered (non-FR) furniture to determine the number of PAHs released by the burning materials. In addition to measuring pure PAH release from the materials, the team assigned multiple PAHs "toxicity values" to quantify their carcinogenic risk compared to benzo[a]pyrene which has the toxicity value 1.0. The g/kg measurement of the toxicity values was divided by the total PAH yield to calculate a "Toxicity Index" in order to more easily determine the toxic quality of the smoke. One notable type of furniture tested

was sofas, a common type of furniture found in a typical housefire. Non-FR sofa burns generated 41g/kg PAH with a Toxicity Index of .016. Phosphorous-FR and Bromine-FR sofas generated 67 and 153g/kg with toxicities of .013 and .012 respectively. FR furniture is common in households despite its smoke toxicity due to preference of its ability to slow the progress of fires once they occur.

Research has also been conducted to determine how PAHs transfer from a fire to a firefighter's skin. In a 2020 study by Lao et al., it was determined that barbecue smoke also produces PAHs. In this experiment, participants barbecue meat at an indoor barbecue using a single grill. During the barbecue, air samples were collected by a door and open window alongside a general collection for background air. At each location, air sample collection was performed using a Micro-Orifice Uniform Deposit Impactor (MOUDI) with 47-mm diameter glass microfiber filters end-connected to polyurethane foam. The MOUDI samplers collected samples at a constant flow rate of 30 L min⁻¹. Of particular interest to Lao et al. was how exactly PAHs contaminated exposed skin, singling out the particulate matter (PM) expelled in smoke as a potential vector for transmission. Study of the barbecue air revealed that most PM formed was either >18µm or <1.8µm, with fewer particles produced between. It was also determined that the PM formed by pre-loading meat was much smaller than PM generated once food was placed on the grill. PAHs bound to PM rather than being in the gas phase were determined to be 4.2, 595, and 639 ng m⁻³ for background air, the door, and the window respectively. For PAHs bound to PM, fine (<1.8µm) particles carried more than coarse (>18µm) particles. Additionally, fine particle-bound PAHs were estimated to deposit more onto skin than coarse particles at 980 ng versus 820 ng. This suggests that PM are a viable vector for harmful PAHs to

enter inside the human body, as fine PM are small enough to enter through hair follicles and potentially bypass the epidermal layer. One proposed optimal nanoparticle size range for follicle-transport is 400 – 700 nm (Schneider et al., 2009). Roughly 20% of PM for both the background air and BBQ fume were produced in this size range, making absorption via follicular pathways a viable future area of study.

Firefighter Hoods

Hoods are essential in mitigating the effects of PAH contamination, as they provide a physical barrier between the skin and PAHs in the air. According to Keir et al. (2017), firefighters who experienced the most absorption were those who took part in vertical ventilations and those who did not wear their hoods. Current turnout gear hoods are successful in protecting the firefighter from burning, but the maintenance and decontamination are questionable. Nazare et al. (2014) tested the mechanical protective qualities of turnout gear fabrics with melamine fiber threads. The primary protective qualities measured in the experiment were tensile strength, tear resistance, and thermal protection of the outer shell fabrics after aging under ultraviolet (UV) light, laundering, abrasion, and heat exposure. This study constructed four outer shell fabrics of 40% melamine and 60% para-aramid fibers labeled BK-00, BK, BBK, and BKP. BK-00 and BK are identical in composition and fabrication except that BK-00 was never exposed to a water repellent finish. BBK was treated with a durable water repellent finish, and BKP was constructed with a basket weave rather than a plain weave. BK-00's tear strength prior to any treatment was the highest of the four fibers, but after full treatment was the lowest. Nazare et al. concluded that UV exposure has the highest effect on lowering tear resistance, with laundering playing a significant role in diminishing tear resistance. UV

exposure also had the greatest effect in reducing the tensile strength of each fabric. BBK retained the most tensile strength post-UV-exposure and BK-00 retained tensile strength the least. For thermal protectiveness, BBK had the highest rating prior to any exposure testing. Post-exposure, BK and BKP retained a higher level of thermal protectiveness.

Once hoods are exposed to dangerous air-borne chemicals, it is necessary to decontaminate them for safe reuse. Research is currently ongoing about the effectiveness of various detergents and cleaning methods for turnout gear; but research has shown that it is possible to have a 56-81% decrease in contamination with laundering (Mayer et al. 2019).

CHAPTER THREE

Methodology

To test the smoke-borne PAH filtration ability of firefighter hoods, we adopted a methodology inspired by the methodology of Parker et al. (2018). Parker et al. constructed a dual stream laboratory-scale smoker which ran smoke through a zeolite filter and a control column filled with ceramic granules and sand. As detailed in the following section, the main difference in our smoker is that smoke will be passed through a layer of firefighter hood fabric and an open-air control to simulate the effective protection of wearing and not wearing a hood.

Filtration Experiment

To create smoke, we constructed a rudimentary smoking rig according to modified specifications in Parker et al. (2018) under a hood. A 1L ThermoFisher filter flask was placed onto a hot plate and filled with hickory pellets. Air was supplied to this flask via an air compressor at approximately 1-3 psi. The wood flask was connected to a separate 1L flask via vinyl tubing. This second flask was submerged in an ice bath to operate as a condenser. The output of this flask was connected via tubing to a splitter. The splitter allowed smoke to pass through one of two pathways; an unfiltered control pathway and a pathway covered by an Ara-Tek FR™ Tri-Blend Hood sample. Each pathway terminated into a separate beaker containing 40mL of water sitting in an ice bath. All openings and tubing joints were secured using several layers of heavy-duty tape.

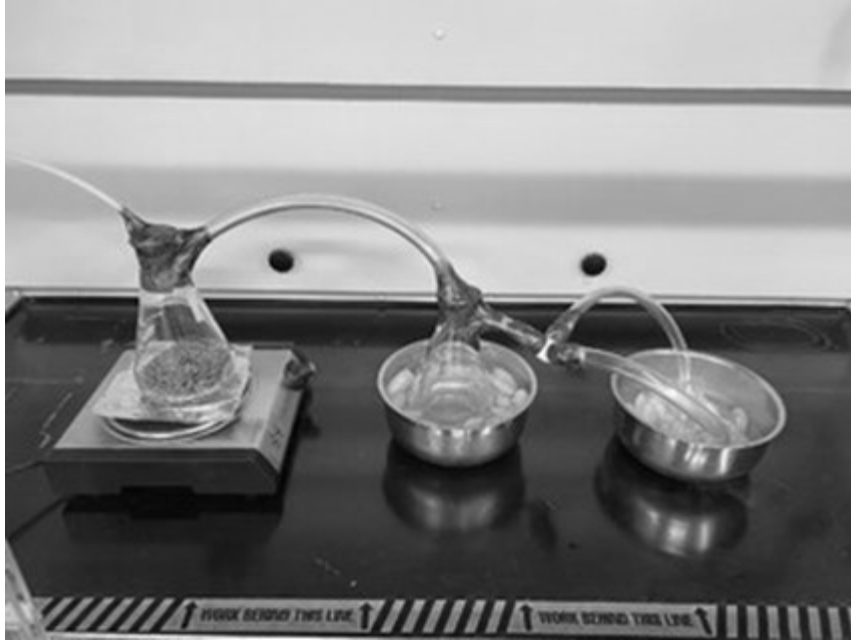


Figure 1. Smoking Rig Prior to Testing

Two separate burns were conducted. During the first burn, 100.200g of wood was placed within the burn flask. The experiment was allowed to run for 15 minutes. After cleaning and replacing the tubing in the rig, a second burn was conducted with 150.012g of hickory pellets. Three more hood samples were tested during this second burn. Each sample was filtered for approximately 15 minutes. At the end of each run, the air compressor was switched off to allow for easier replacement of the hood and collection beakers.



Figure 2. Smoke Filtration in Progress

The PAH extraction methodology similarly follows the method laid out by Parker et al. (2018). After smoking, the collection beakers were treated with 22 mL of methanol. To prepare for the extraction of PAHs from the water, HyperSep C18 SPE cartridges were conditioned with 10 mL methanol followed by 10 mL water-methanol at a 65:35 v/v ratio. After running smoke water samples through cartridges, each was washed with 15 mL water followed by 5 mL of water-methanol. Each cartridge was allowed to gravity-dry while we monitored the smoke. PAHs were eluted from SPE cartridges using 4 mL of cyclohexane and stored at -80°C for further GC-MS analysis. Unfiltered samples were labeled with the number of their run and “A” while the hood-filtered samples were labeled as “B”.

GC-MS Analysis

A DSQ II Mass Spectrometer (Thermo Scientific) was prepared for the separation and identification of collected samples. The mass spectrometer was equipped with a Trace GC Ultra Gas Chromatograph and a TriPlus autosampler, using a 60 m gas chromatography column with an internal diameter of 0.25 mm. The standard for detecting PAHs was SpexPrep PAH Mix A (Lot #AA19021102). Samples 1A, 1B, 2B, and 3B were phase-separated, so the cyclohexane phase of each of these was transferred to airtight GC vials. The vial containing Sample 2A was broken upon arrival to the GC-MS lab, so no data could be collected. 1 μ L of present samples were injected in splitless mode into the instrument. The column was started at 50 °C and ramped up by 10°/minute to 300 °C. After separation, samples were introduced into the mass spectrometer via electron ionization. Data were acquired in the range of 50 to 500 m/z.

The Xcalibur Qual Browser software (Thermo Scientific) was utilized to assist in analysis of raw data. The data of each chromatographic peak was summed and the background signal subtracted to collect a mass spectrum. This spectrum was then searched against the software's built-in NIST library to determine the most probable compound identity. This method was used to verify the peaks in the PAH standard as well.

CHAPTER FOUR

Results

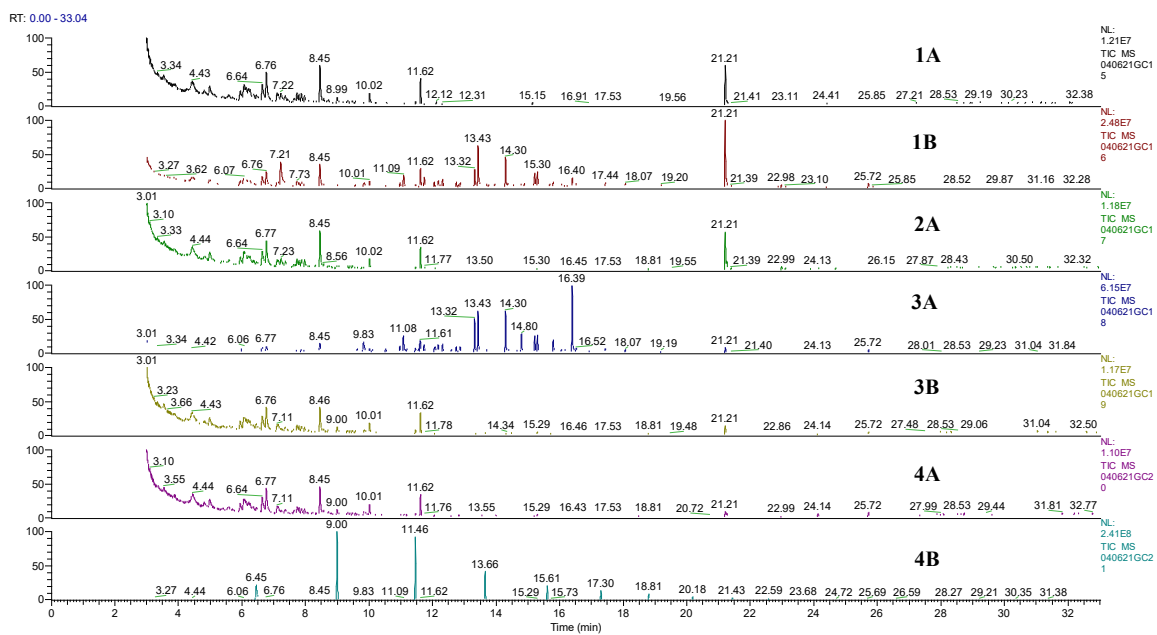


Figure 3. Side-by-Side Comparison of Sample Chromatograms 1A (Top) to 4B (Bottom)

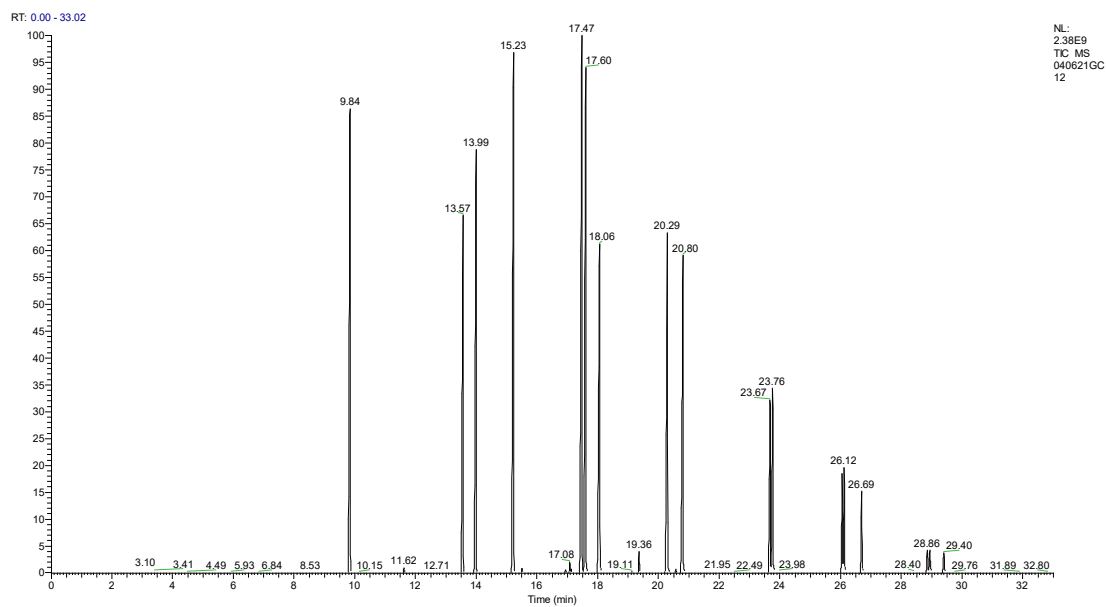


Figure 4. Chromatogram of PAH Standard Mix

Table 1. Sample Peak Identification Table with Select Probabilities

Name	Retention Time Range (min)	Probability
Nonane	4.96 – 5.02	19.89
Benzene, 1-ethyl-3-methyl-	6.04 – 6.10	23.48
Cyclotetrasiloxane, octamethyl-	6.43 – 6.47	80.09
Benzene, 1,2,4-trimethyl-	6.61 – 6.66	24.12
1-Hexanol, 2-ethyl	7.20 – 7.25	33.23
Undecane	8.43 – 8.49	26.59
Cyclopentasiloxane, decamethyl-	8.98 – 9.00	93.38
1H-indene, 1-methylene-	9.81 – 9.84	32.87
Dodecane	10.00 – 10.02	16.99
Benzeneethanamine, 2,5-dimethoxy-a-methyl	10.50 – 10.53	42.14
3,5-Dimethoxytoluene	10.94 – 10.99	51.64
Phenol, 4-ethyl-2-methoxyl-	11.06 – 11.10	56.60
Cyclohexasiloxane, dodecamethyl-	11.44 – 11.48	97.02
Benzocycloheptatriene	11.44 – 11.47	13.09
2-Methoxy-4-vinylphenol	11.60 – 11.62	39.27
2(3H)-Furanone, 5-butyldihydro-4-methyl, cis-	11.72 – 11.74	36.47
Benzaldehyde, 2,3-dimethoxy-	12.04 – 12.08	11.41
3-Allyl-6-methoxyphenl	12.16 – 12.20	16.89
Phenol, 2-methoxy-4-propyl	12.30 – 12.33	53.63
Benzene, 1,2,3-trimethoxy-5-methyl-	12.72 – 12.75	75.49
Phenol, 2-methoxy-4-(1-propenyl)-	12.85 – 12.88	16.57
	13.41 – 13.45	30.17
2,5-Dimethoxybenzyl alcohol	13.31 – 13.33	32.17
Cycloheptasiloxane, tetradecamethyl-	13.64 – 13.67	64.78
5-tert-Butylpyrogallol	14.28 – 14.31	26.75
2,5-Dimethoxy-4-ethylamphetamine	14.78 – 14.81	41.50
Pentanoic acid, 2,2,4-trimethyl-3carboxyisopropyl ester	15.13 – 15.17	65.46
Phenol, 2,6-dimethoxy-4-(2-propenyl)-	15.20 – 15.23	85.47
	15.78 – 15.81	67.56
	16.38 – 16.41	80.50
2,4-Hexadienic acid, 3,4-diethyl-, dimethyl ester	15.29 – 15.32	32.67
Cyclooctasiloxane, hexadecamethyl-	15.60 – 15.62	95.52
Cyclonasiloxane, octadecamethyl-	17.29 – 17.31	87.03
	18.79 – 18.82	39.55
	21.41 – 21.45	64.27
	22.57 – 22.61	59.14
	23.66 – 23.70	55.17
	24.69 – 24.73	35.89
2,3-Dimethoxy-5-aminocinnamotrile	18.05 – 18.08	34.81
Butyl citrate	21.19 – 21.23	76.22
1H,15H-hexadecamethyloctasiloxane	20.17 – 20.20	36.73
Hexadecanoic acid, butyl ester	21.25 – 21.28	66.23
Phthalic acid, di(oct-3-yl) ester	24.12 – 24.14	11.97
1,4-Benzenedicarboxylic acid, bis(2-ethylhexyl) ester	25.70 – 25.72	50.08

For ease of comparison, the chromatograms representing the separation of compounds within the samples have been positioned atop one another in Figure 3. Note that the 2nd control sample, 2A, was unfortunately broken during transit and was therefore unable to be injected into the instrument. The mass to charge ratios generated by the mass spectrometer for each discernable peak in Figure 3 were cross-referenced with an NIST library to generate Table 3, where the probability value represents the similarity between the collected mass spectra for a peak and the expected mass spectrum. Values approaching 100 indicate a higher degree of similarity and therefore are more likely to be the compound identified.

CHAPTER FIVE

Discussion

We were surprised to find that the sample chromatograms in Figure 3 and the standard chromatogram in Figure 4 do not match up. The lack of any PAHs in Table 3 identifiable via retention times and m/z further suggests that we were unable to either capture PAHs in the water or extract them using the SPE columns. However, it is possible to identify some key chemical contaminants which otherwise should not be in the water that have made their way to the GC-MS.

In the chromatograms for 1A, 2A, and 2B, a large peak at 21.21 minutes was identified as belonging to butyl citrate with a probability of 76.22. Butyl citrate has many industrial and commercial uses as a solvent and plasticizer. According to the European Chemicals Agency, butyl citrate poses some danger for aquatic life and is notably corrosive when in contact with eyes. The presence of this compound in both the filtered and unfiltered samples suggests that firefighter hoods are fairly permeable to similar compounds, and the lack of butyl citrate in the 3 and 4 series of samples suggests that this compound was present in the hickory pellets and had largely smoked out by the collection of these samples.

Interestingly, there is a substantial peak in 4B relating to decamethyl-cyclopentasiloxane at 93.38 probability. This peak is present in the other chromatograms but not nearly at the same intensity as in 4B, a filtered sample. This compound contains a wide variety of industrial and agricultural uses and is sometimes used as a component in detergent. It may be possible that decamethyl-cyclopentasiloxane may have off-gassed

from the 4B hood sample into the water, which could suggest that chemicals adherent to the surface of hoods have the ability to transfer onto the wearer during a fire. Further studies into the efficacy of washing firefighter equipment should be conducted to ensure hoods are free of contaminants before use.

The presence of compounds in both the filtered and unfiltered chromatograms and the lack of a decrease in intensity in the former implies that firefighter hoods are imperfect chemical filters. While more than functional in protecting firefighters from burns, hood use may still leave the neck at risk of absorbing smoke-borne chemicals. The specific PAH absorption and permeability of the hoods cannot be determined with the data in this report, but it is possible to recognize areas of improvement that could allow this to serve as a preliminary experiment.

Experimental Limitations and Areas for Improvement

There are several factors which may have led the inability to isolate PAHs in our samples and determine the hoods' absorptive abilities. The first area of scrutiny is the hood smoker. As visible in Figures 1 and 2, the construction of our smoker could improve in its design. We were able to keep smoke loss relatively low, and the air pump helped the smoke rush through the rig to bubble into both collection beakers, but the smoker could certainly be made more efficient. Construction of a more seamless, proficient rig could help funnel more smoke towards collection and increase PAH retention.

It is furthermore possible that our choice of fuel for the smoke was impractical for producing PAHs. PAHs are present in nearly all smoke from organic material fires, but it may be possible to optimize PAH production with certain fuel. Parker et al. used wood

chips whereas we used hickory pellets which were readily available. Despite package labeling, it seemed that the pellets were flavored. This could have contributed to some of the other chemicals listed in Table 3. It would be best to use a fuel source which produces as few other contaminants in smoke aside from PAHs. Studies regarding PAH production during burning of certain materials would be valuable for this purpose.

Lastly, reduced PAH concentrations in our collected samples lies in the solid phase extraction. A few of the samples were phase-separated, suggesting improperly dried cartridges prior to eluting with cyclohexane. Without access to a vacuum drying method like Parker et al., we had to rely on gravity drying. Our timeframe and concern of over-drying the cartridges lead to complications with our samples. PAHs are volatile chemicals, and it is very possible that they evaporated while drying in the open air. Additionally, PAHs are incredibly hydrophobic, leading to reduced solubility in water. Although Parker et al. (2018) used water to effectively capture PAHs, it may be beneficial to use a hydrophobic capturing liquid such as an oil. The practice of better technique alongside proper equipment could increase separation efficiency. Furthermore, our SPE cartridges are not the same as those used by Parker et al., but they are marketed as being specifically for the extraction of polycyclic aromatic hydrocarbons. It would have been ideal to run PAH mix through the cartridge to determine effectiveness. Doing this in future experiments, as well as taking time to test other commercially available PAH separation SPE cartridges, may improve the concentration of PAHs in eluted samples.

Carbon Nanomaterial Hoods

Given that there may be an inherent chemical permeability to existing firefighting hoods, one option which may be viable for reducing PAH exposure to the neck could be to experiment with the material composition of the hood. Some carbon nanomaterials, specifically nanotubes, are adept at trapping most PAHs. Yang et al. (2006) observed that nanotubes trap PAHs using radiolabeled pyrene, phenanthrene, and naphthalene alongside the nanotubes SWCNT, MWCNT8, MWCNT15, MWCNT30, and MWCNT50. Their observations with a limited selection of PAHs were that larger nanotubes were more effective at capturing PAHs and that absorption and hydrophobicity of the PAH were correlated. Hu et al. (2020) further confirm that hydrophilic PAHs bind to carbon nanotubes and determined that they exhibited strong binding energies of -7.292 kcal/mol and -6.683 kcal/mol for naphthalene and phenanthrene, respectively.

Another reason why carbon nanotubes are a potential addition to firefighter hoods would be their heat-conducting properties. As summarized by Shahidi et al. (2018), carbon nanotubes conduct heat along the tube axis, which could allow firefighter gear to direct that heat to a cold reservoir. Textiles infused with carbon nanotubes are also more flame retardant and thermally stable than raw textiles. Depending on how effective carbon nanotubes are at preventing dermal exposure to polycyclic aromatic hydrocarbons, infusion of turnout gear with nanotubes could be a long-term and viable improvement to firefighter safety.

CHAPTER SIX

Conclusion

The experiment conducted for this study was not effective in determining the efficacy of firefighter hoods as PAH absorbers, however several other chemicals of concern were identified through analysis. The data obtained provides a foundation for discovery for further research of firefighter health and safety measures. The list of possible observed contaminants suggests that hoods are somewhat ineffective as smoke-borne chemical filters. It would be valuable to attempt a similar experiment analyzing other classes of compounds in smoke such as organophosphate esters, chemicals commonly found in furniture burned in structure fires. Additionally, it is vital to discern new hood materials which can protect the firefighter from burning as well as chemical contamination, such as carbon nanotubule fibers.

APPENDICES

APPENDIX A

PAH Standard Mix Identification

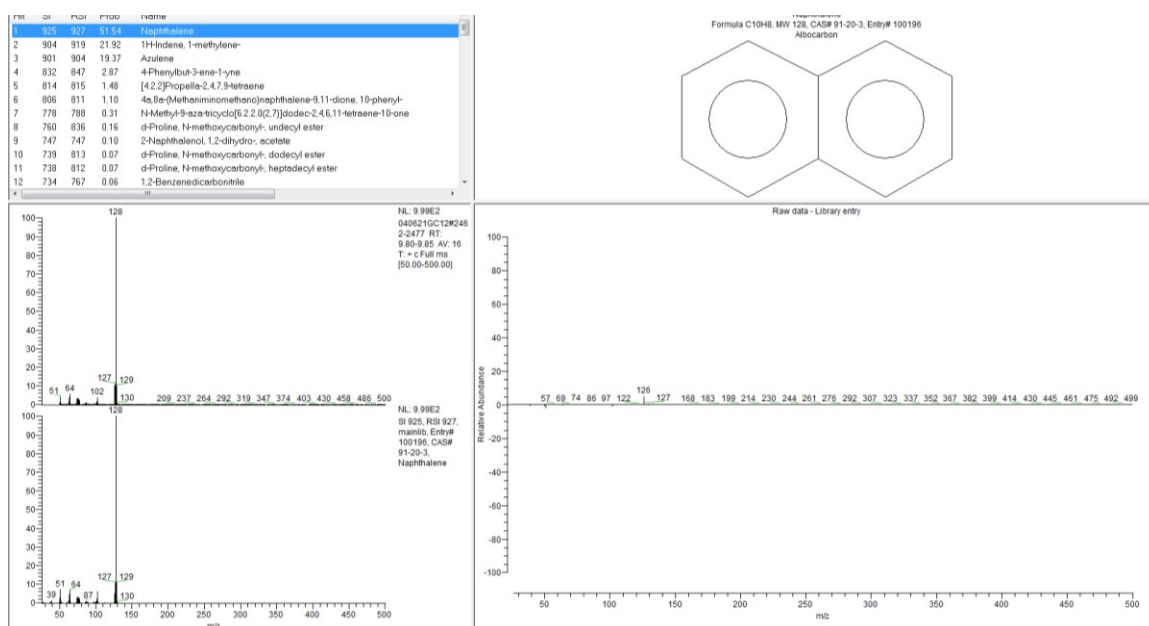


Figure A.1. Identification and Probability of Naphthalene

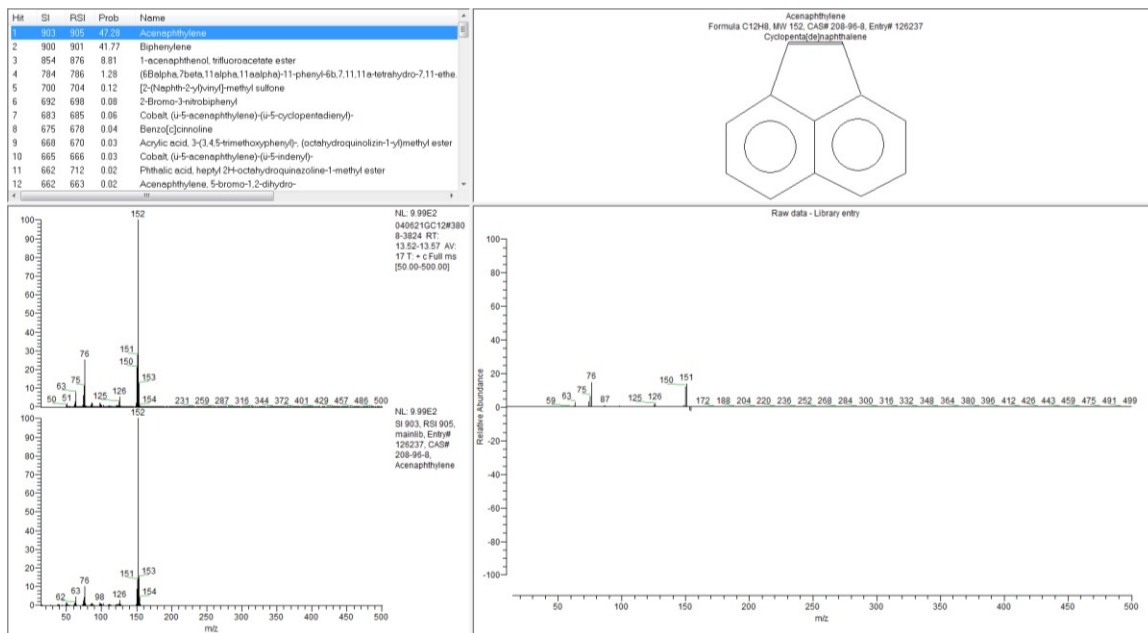


Figure A.2. Identification and Probability of Acenaphthylene

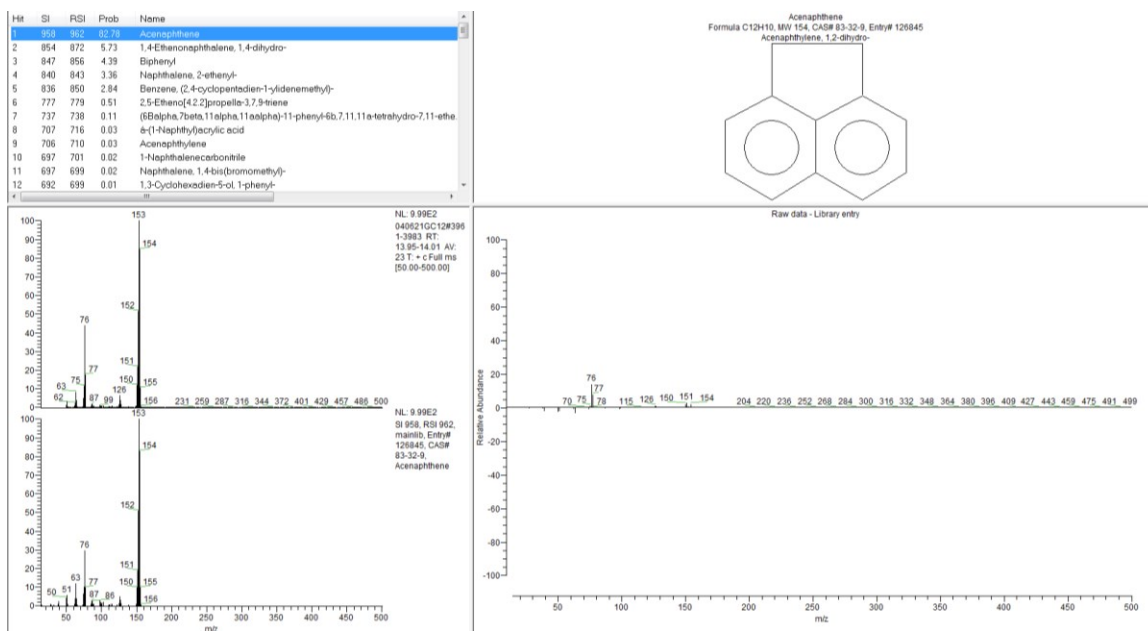


Figure A.3. Identification and Probability of Acenaphthene

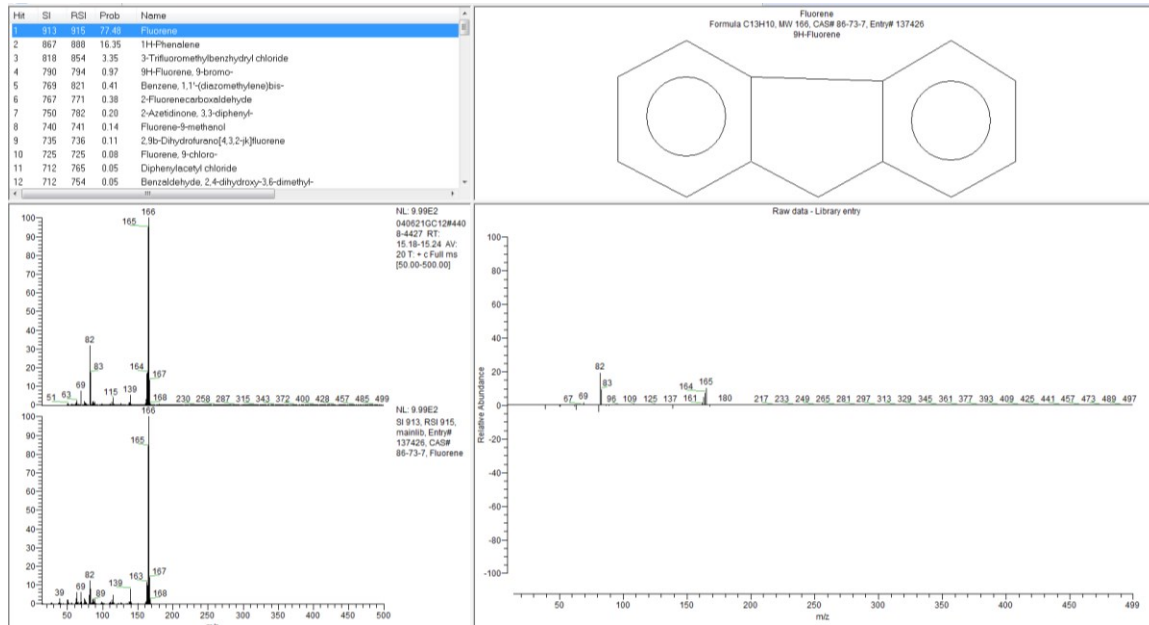


Figure A.4. Identification and Probability of Fluorene

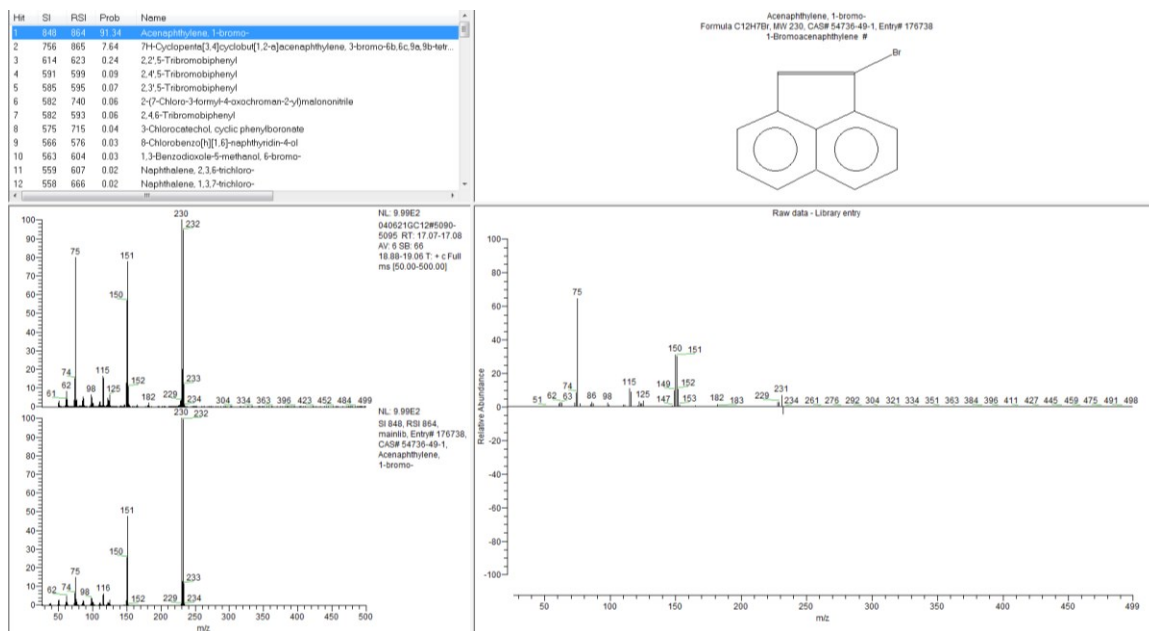


Figure A.5. Identification and Probability of Acenaphthylene, 1-bromo

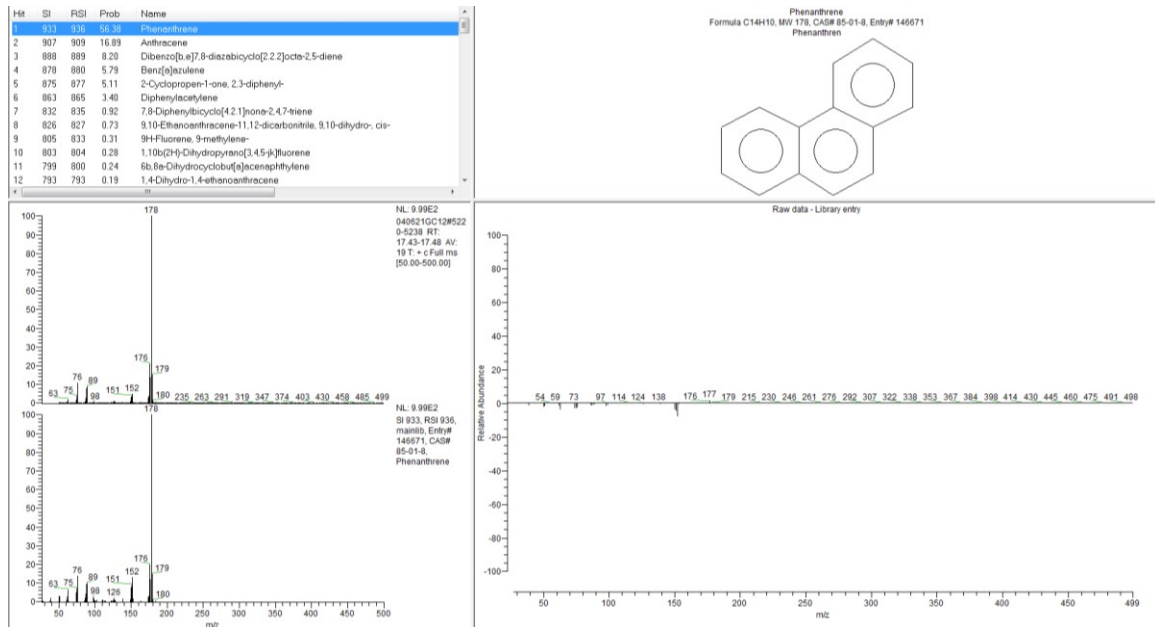


Figure A.6. Identification and Probability of Phenanthrene

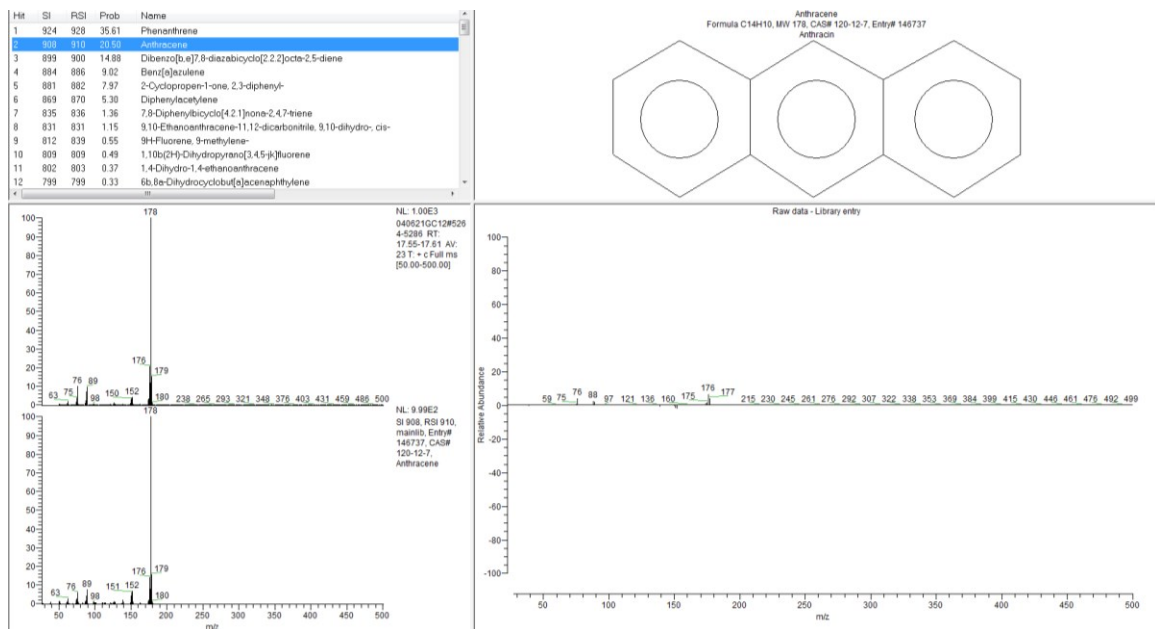


Figure A.7. Identification and Probability of Anthracene

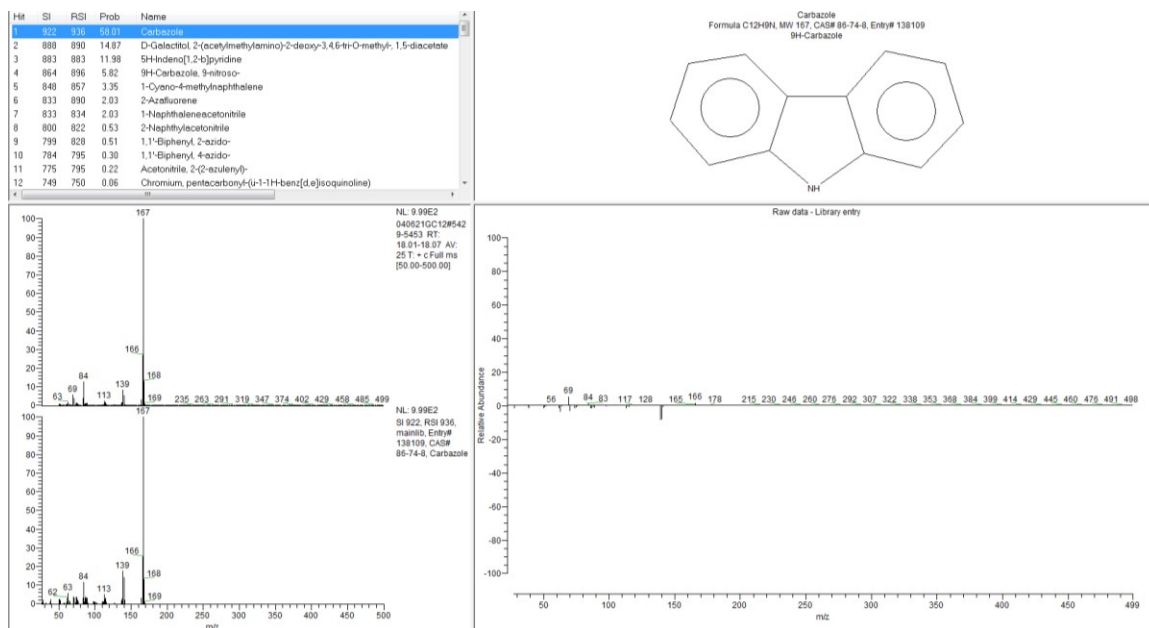


Figure A.8. Identification and Probability of Carbazole

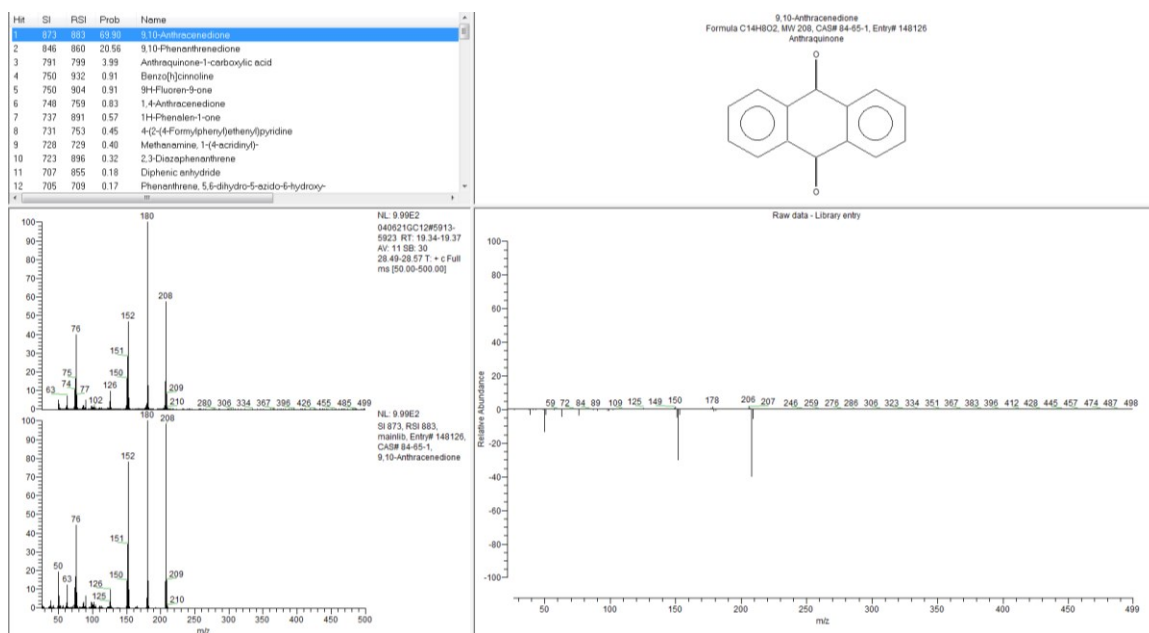


Figure A.9. Identification and Probability of 9,10-Anthracenedione

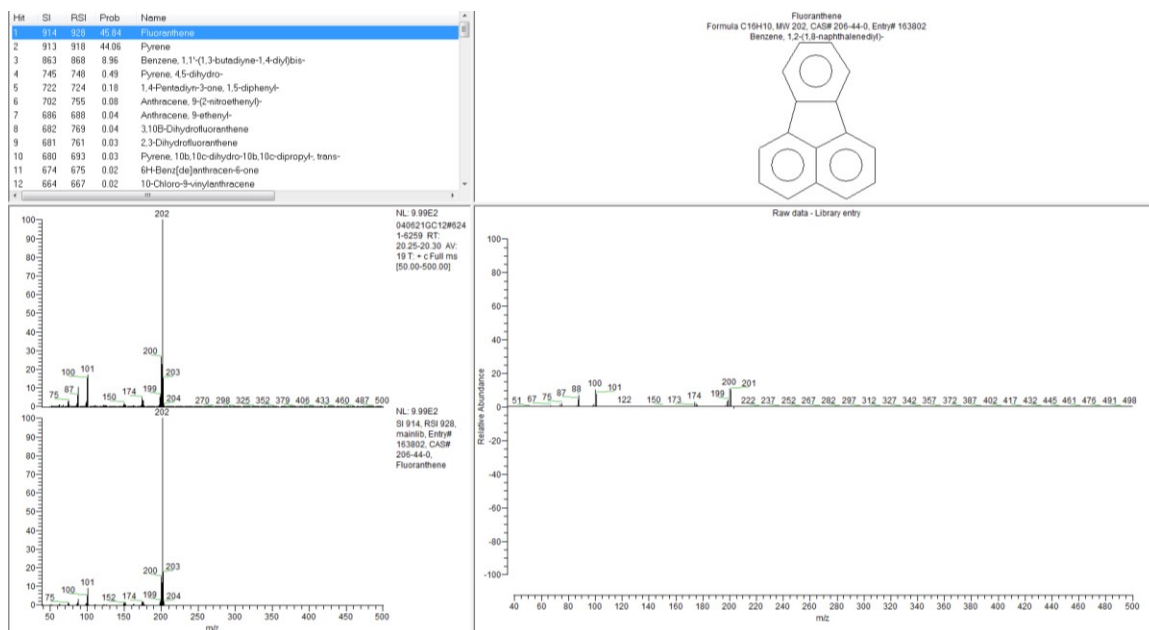


Figure A.10. Identification and Probability of Fluoranthene

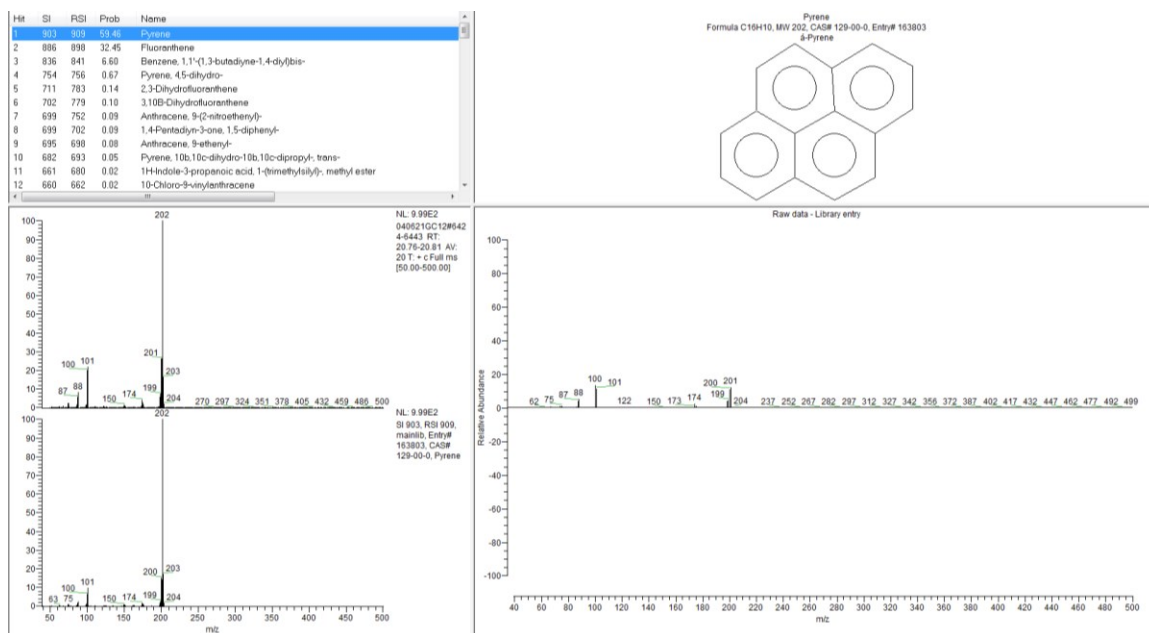


Figure A.11. Identification and Probability of Pyrene

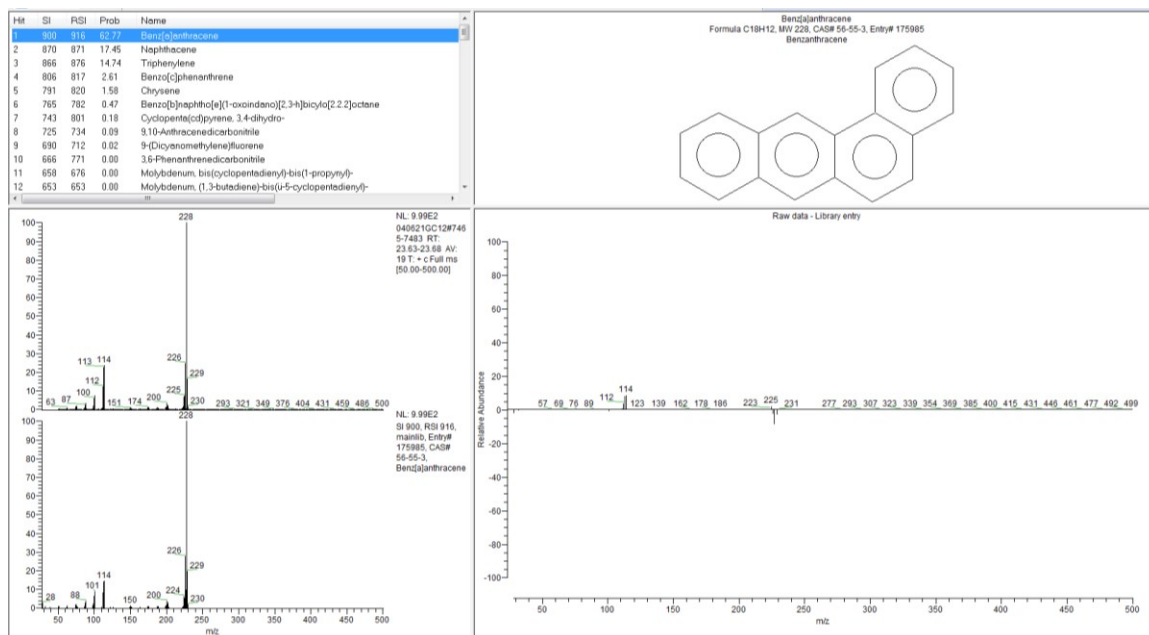


Figure A.12. Identification and Probability of Benz[*a*]anthracene

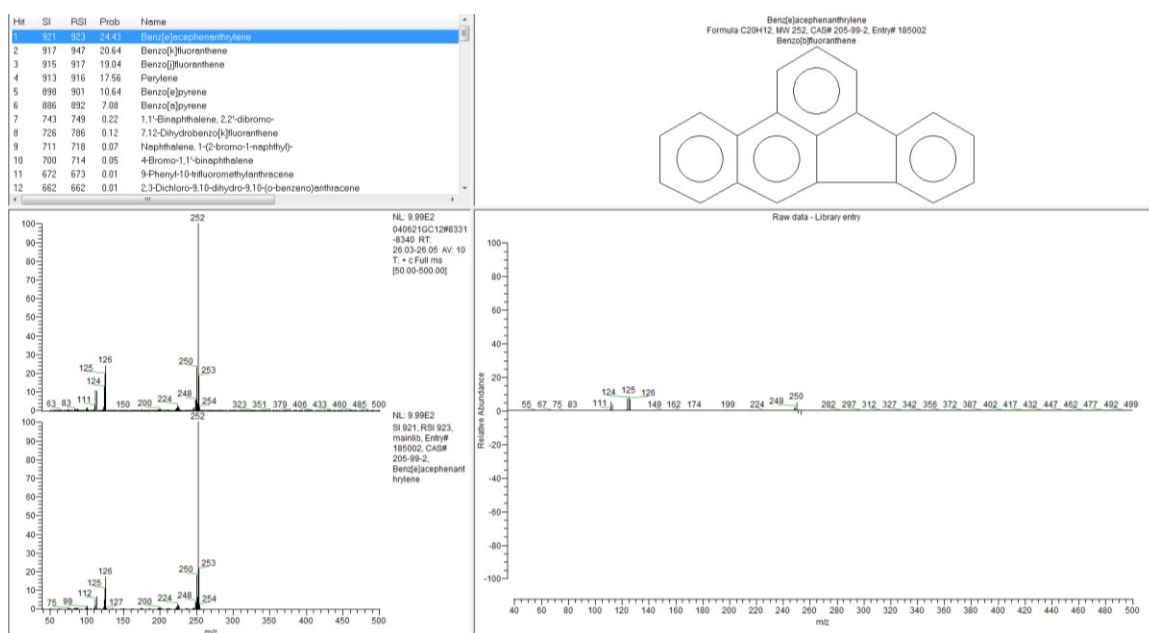


Figure A.13. Identification and Probability of Benz[*e*]acephenanthrylene

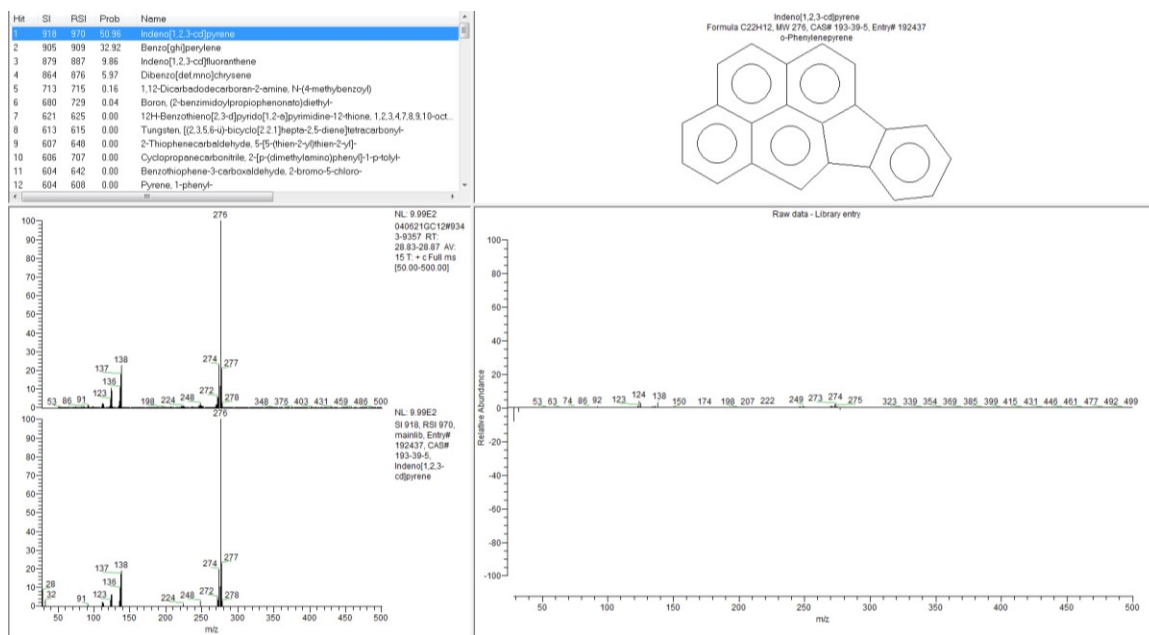


Figure A.14. Identification and Probability of Indole[1,2,3-cd]pyrene at 28.86 Minutes

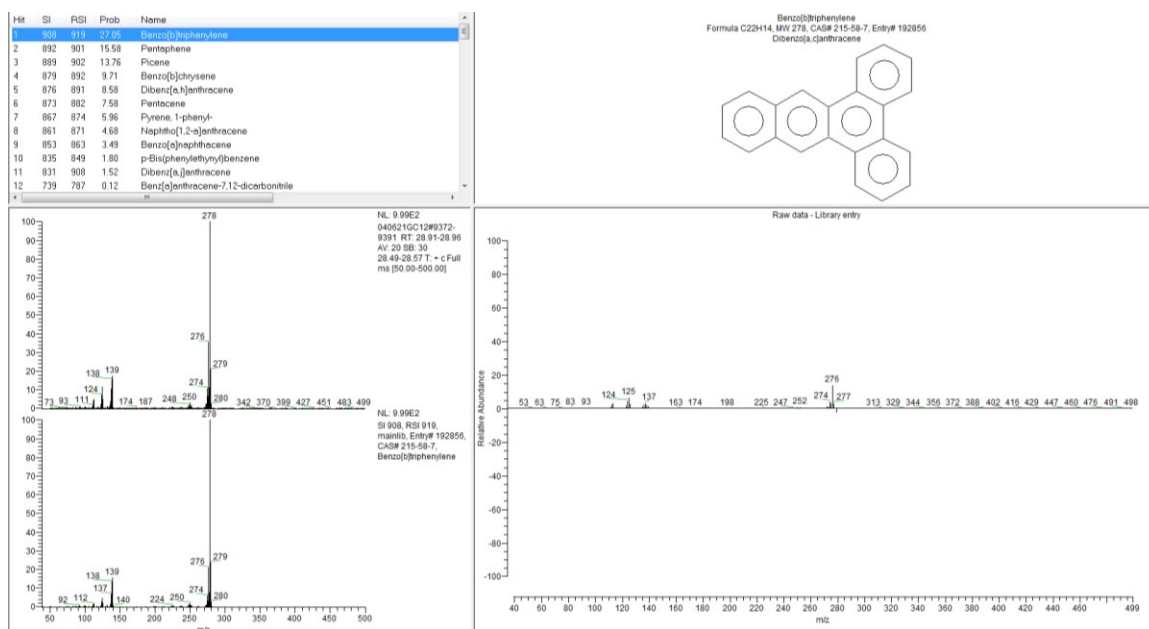


Figure A.15. Identification and Probability of Benzo[b]triphenylene

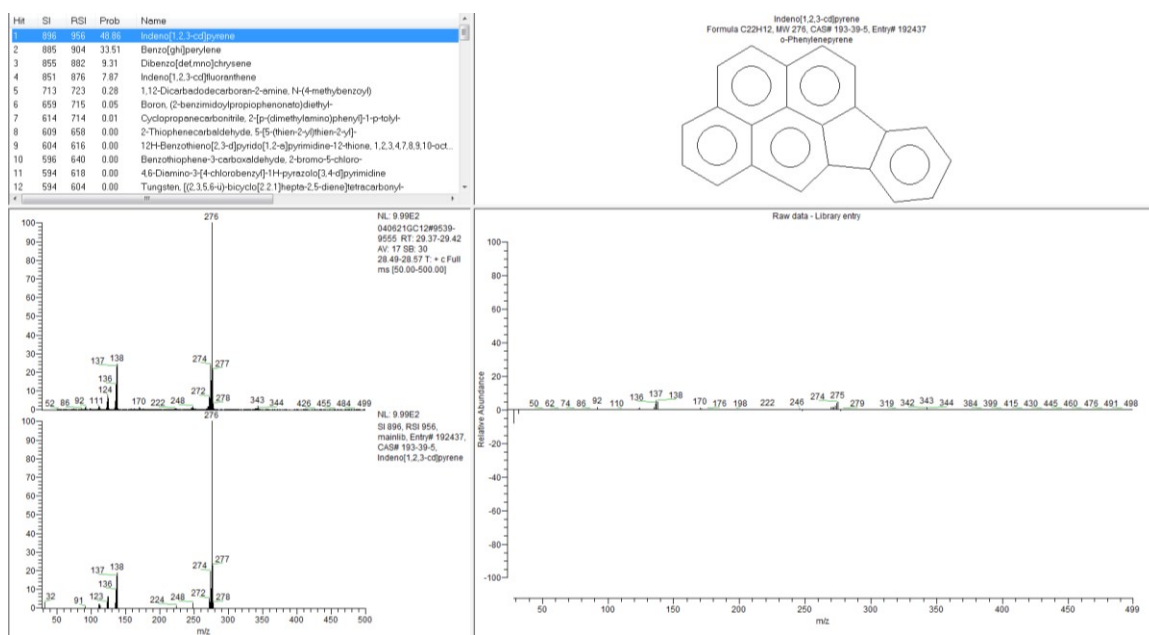


Figure A.16. Identification and Probability of Indole[1,2,3-cd]pyrene at 29.40 Minutes

APPENDIX B

Identification of Table 1 Contaminants

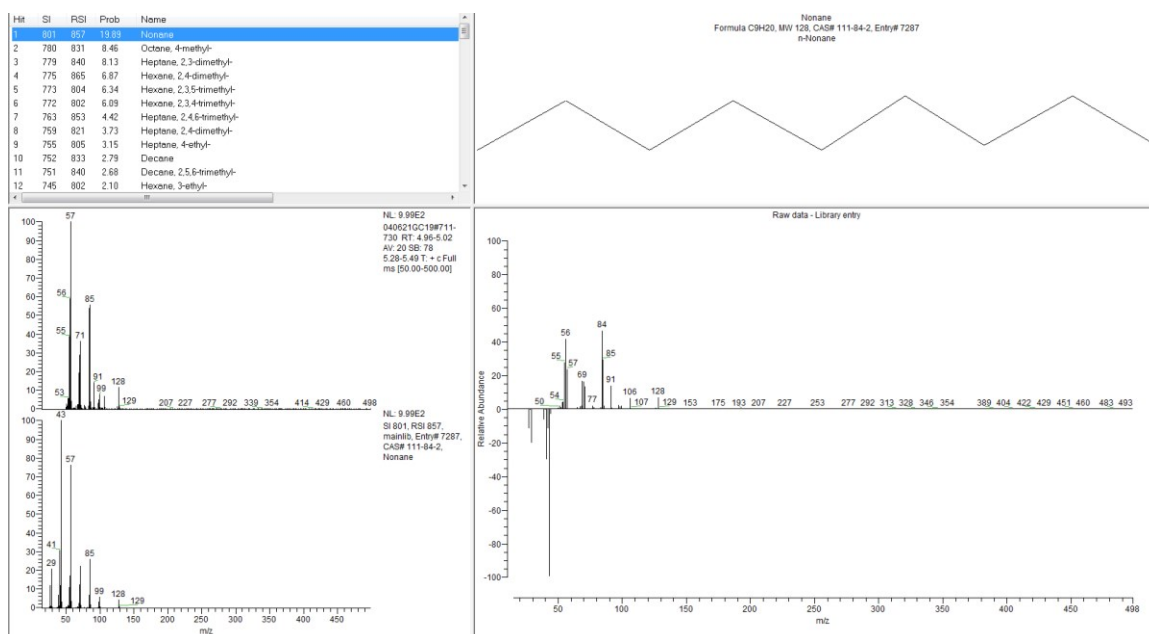


Figure B.1. Identification and Probability of Nonane

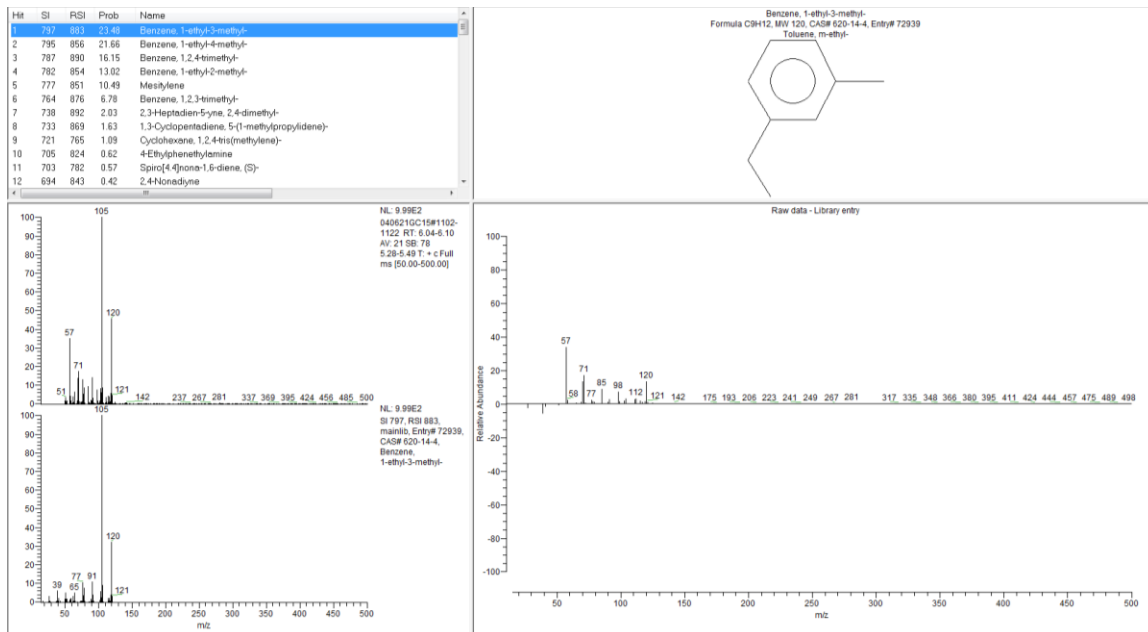


Figure B.2. Identification and Probability of Benzene, 1-ethyl-3-methyl-

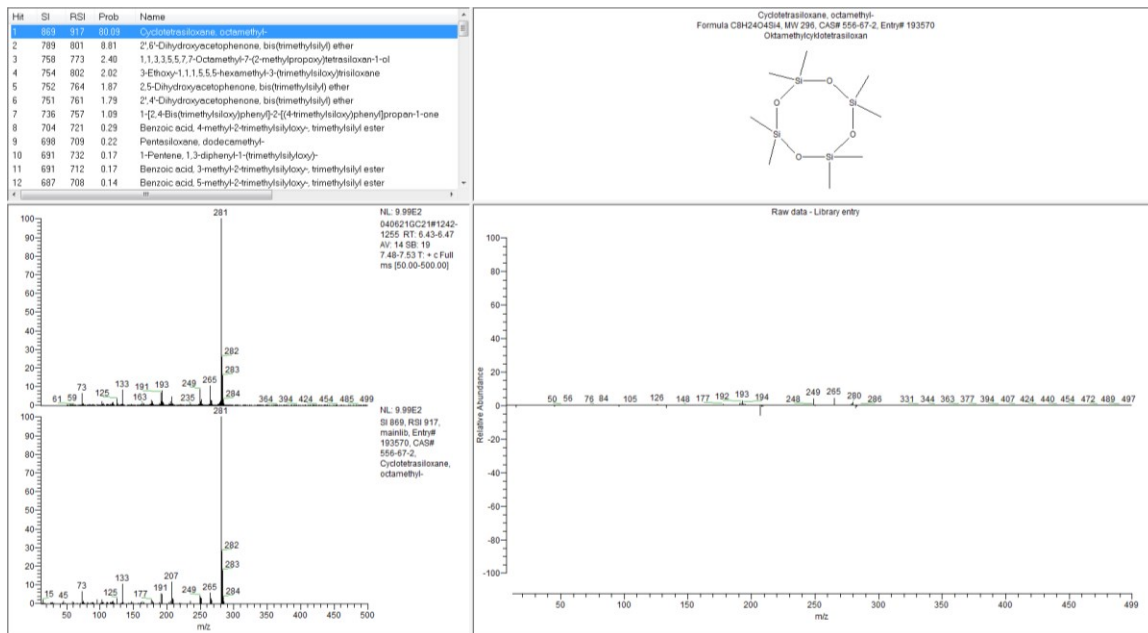


Figure B.3. Identification and Probability of Cyclotetrasiloxane, octamethyl-

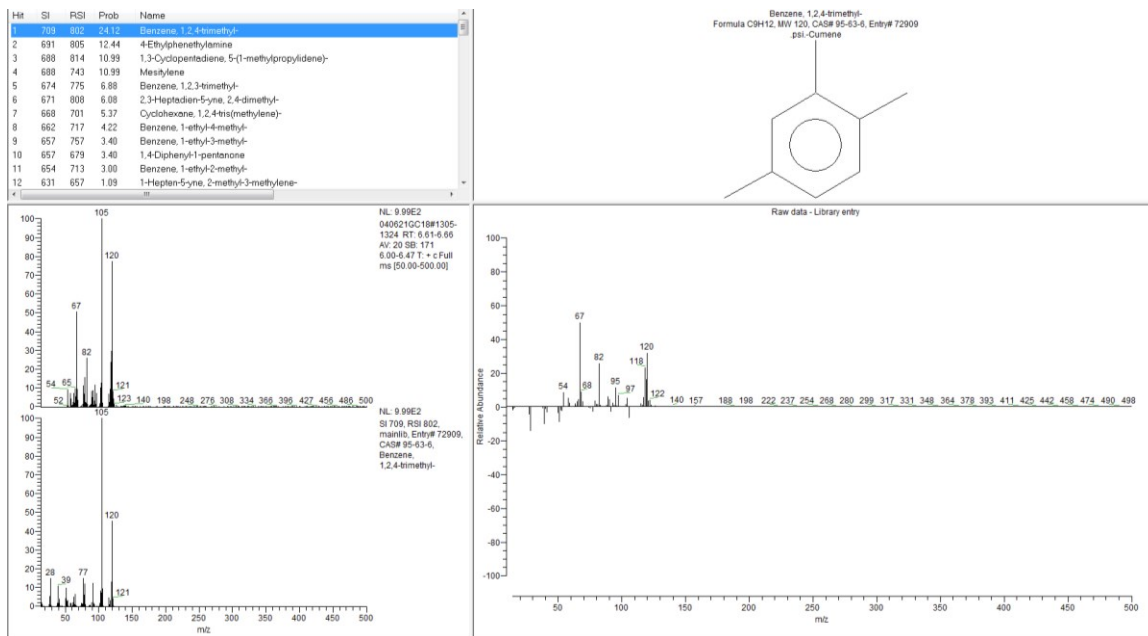


Figure B.4. Identification and Probability of Benzene, 1,2,4-trimethyl-

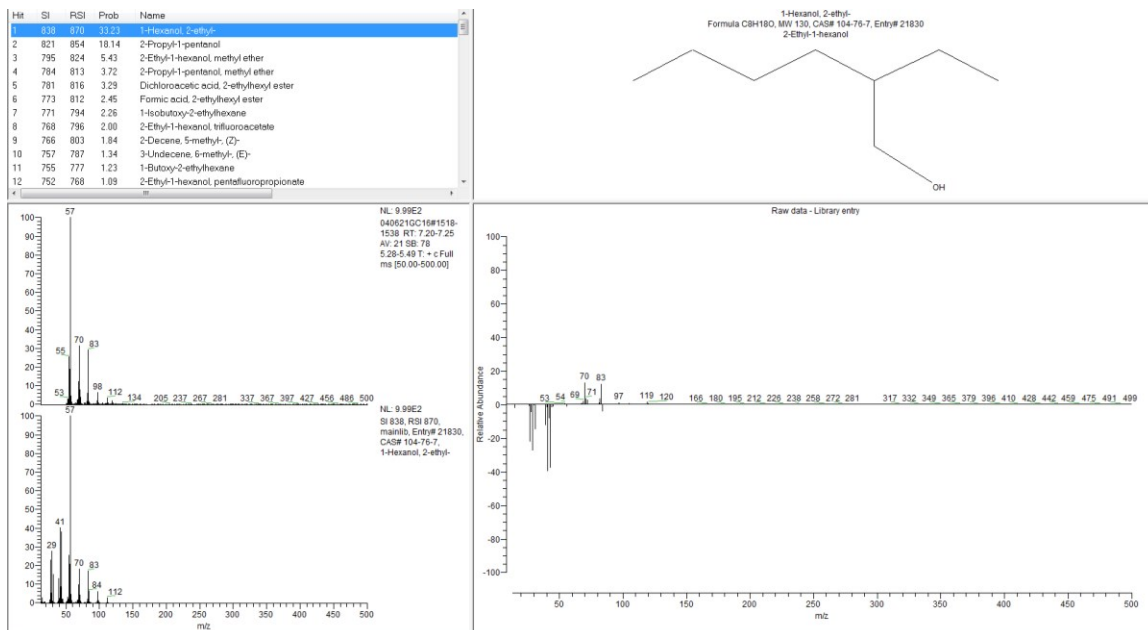


Figure B.5. Identification and Probability of 1-Hexanol, 2-ethyl

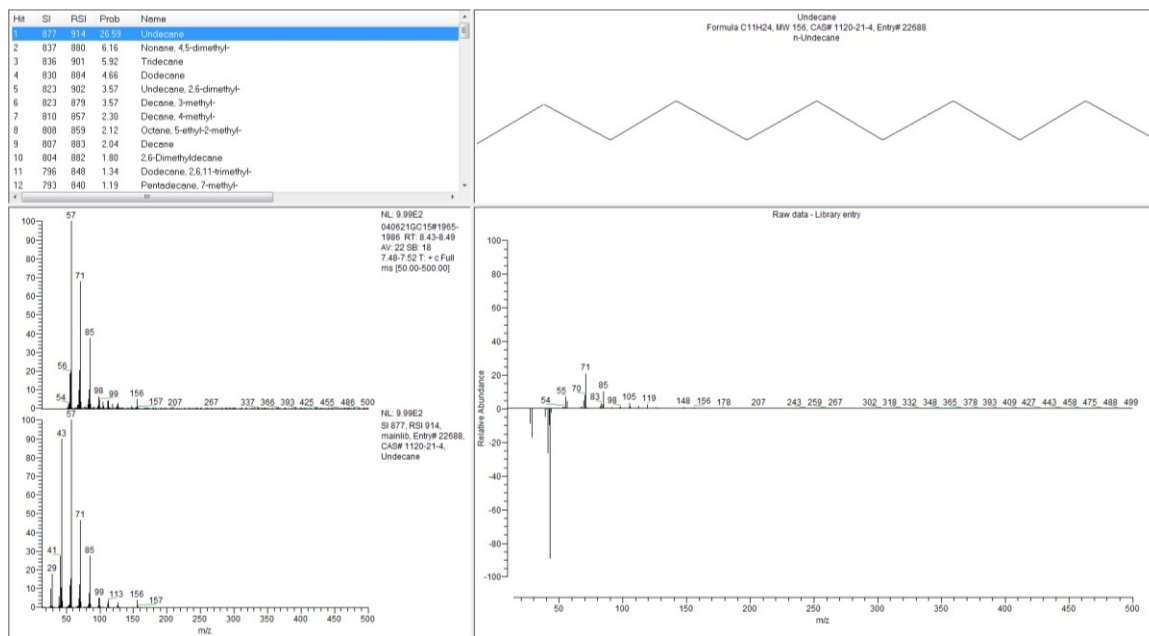


Figure B.6. Identification and Probability of Undecane

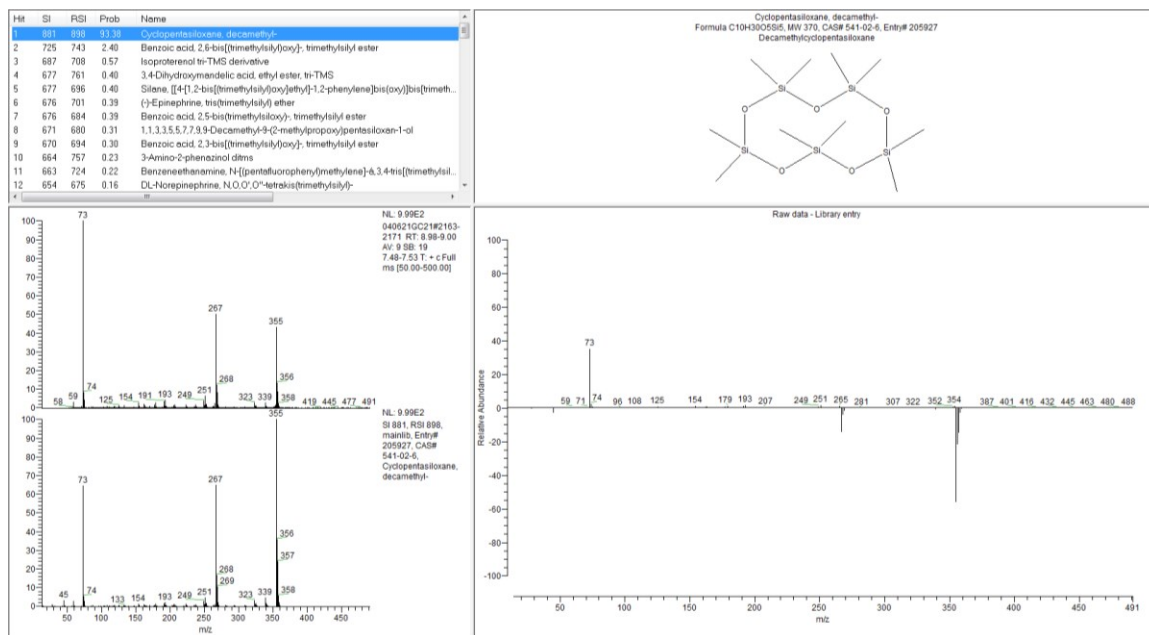


Figure B.7. Identification and Probability of Cyclopentasiloxane, decamethyl-

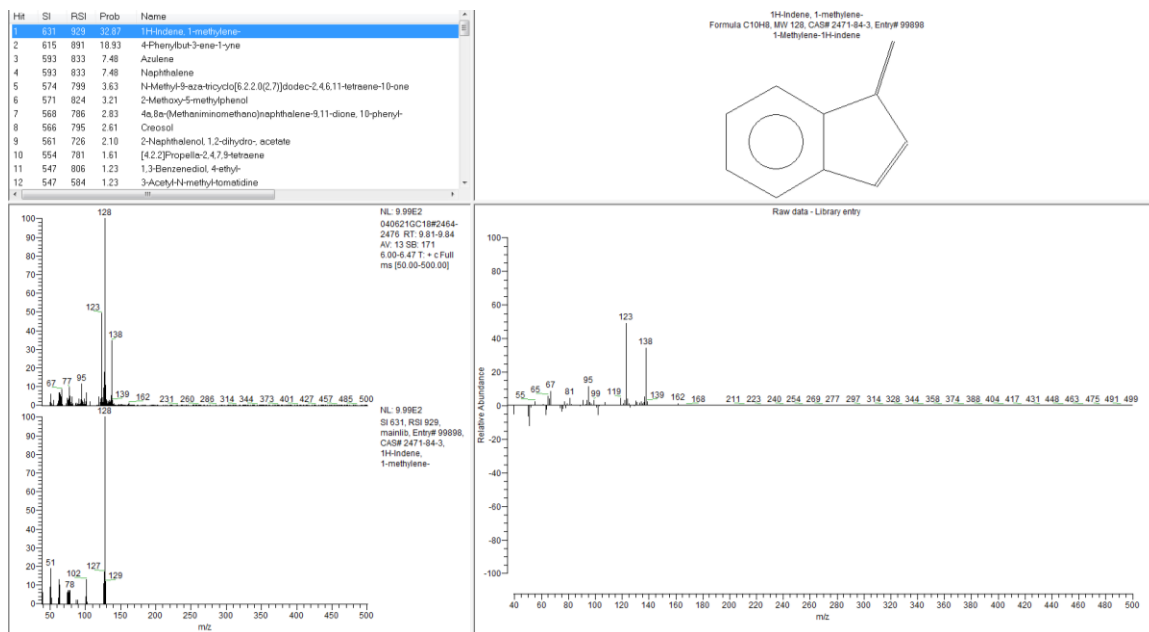


Figure B.8. Identification and Probability of 1H-indene, 1-methylene-

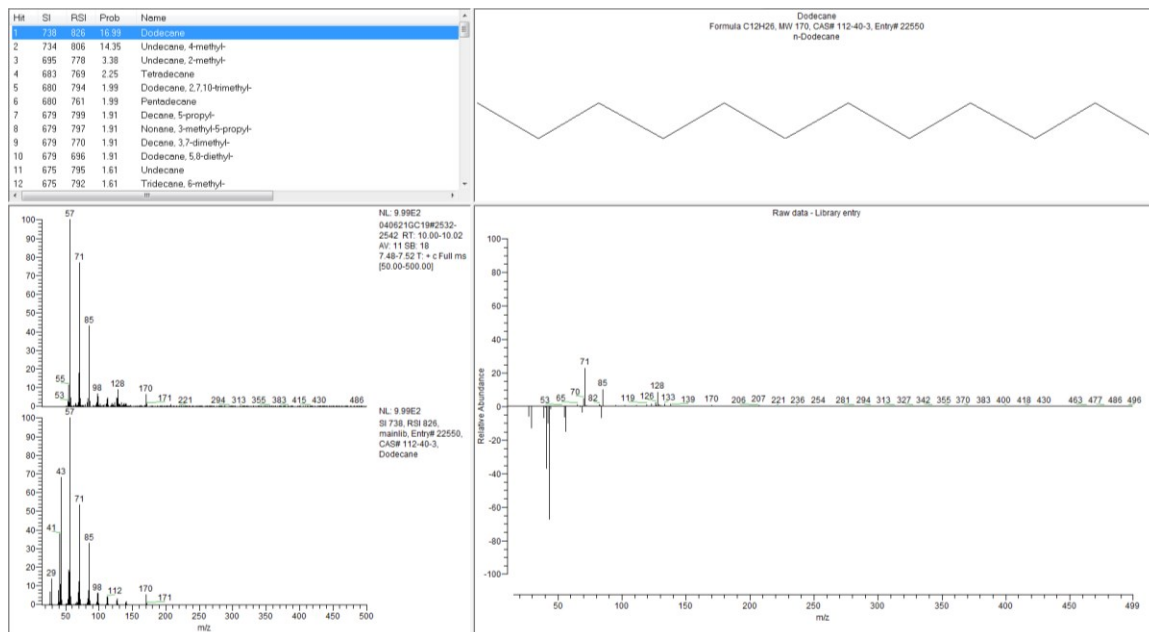


Figure B.9. Identification and Probability of Dodecane

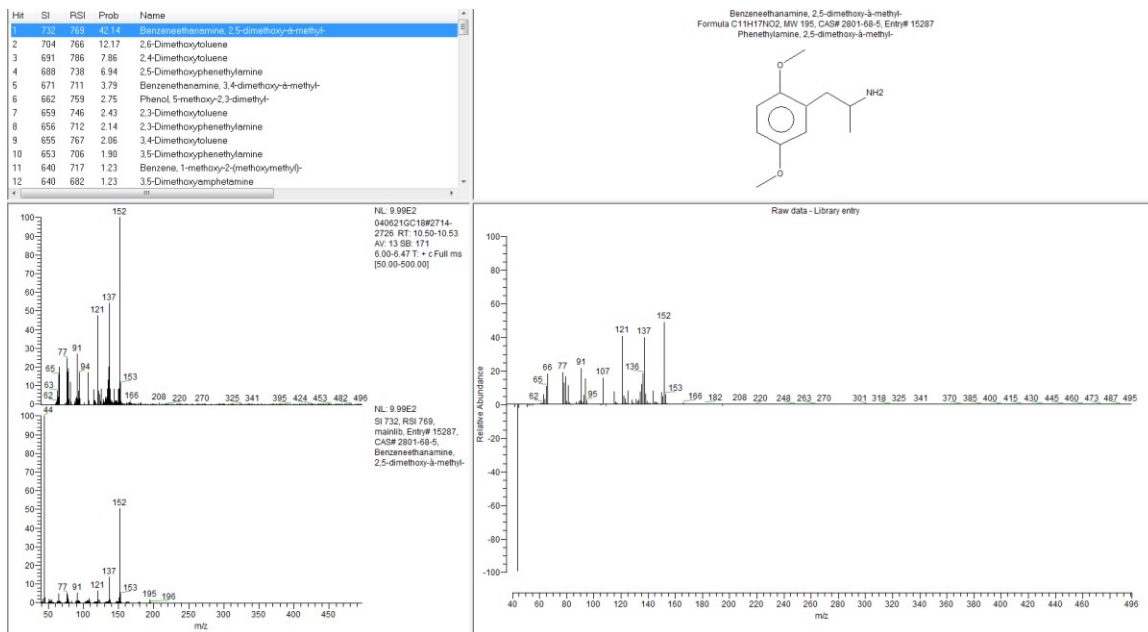


Figure B.10. Identification and Probability of Benzeneethanamine, 2,5-dimethoxy- α -methyl

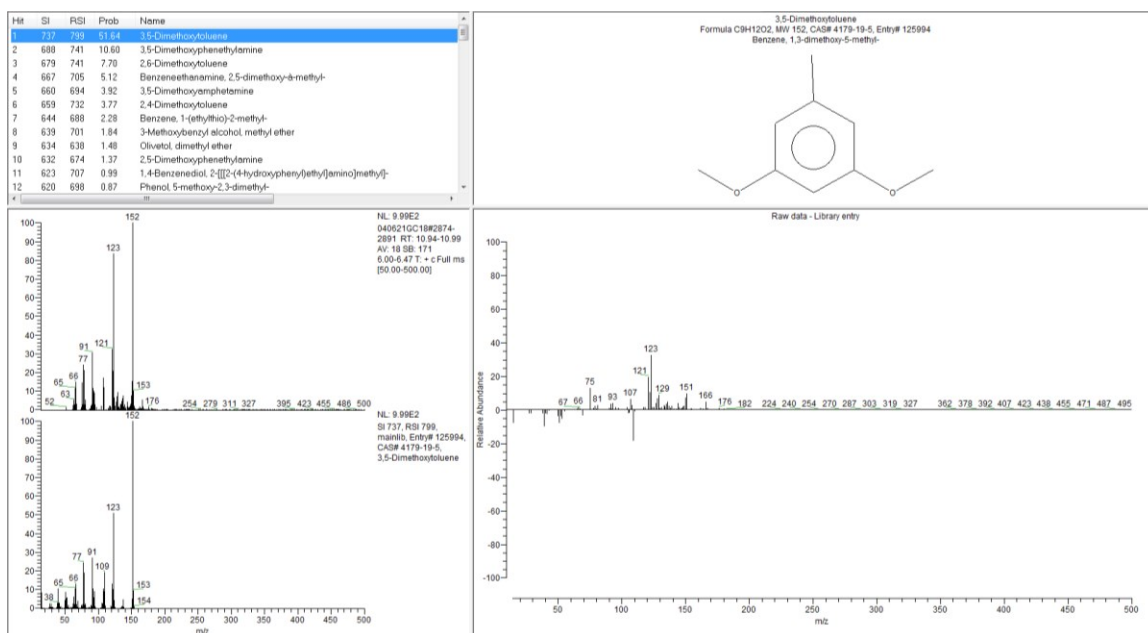


Figure B.11. Identification and Probability of 3,5-Dimethoxytoluene

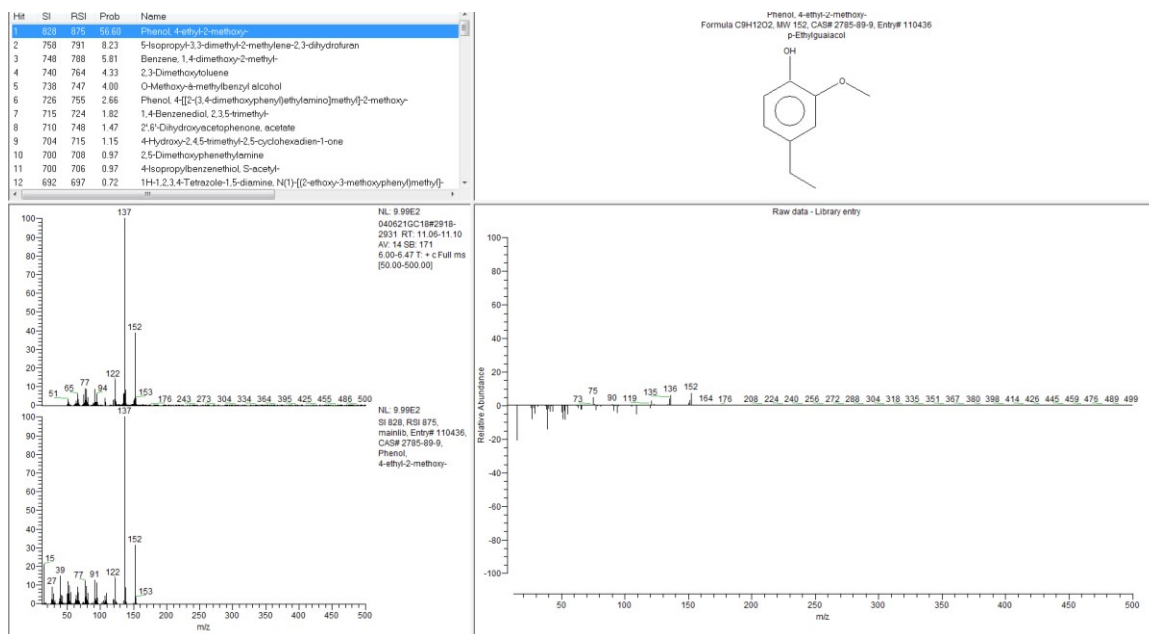


Figure B.12. Identification and Probability of Phenol, 4-ethyl-2-methoxyl-

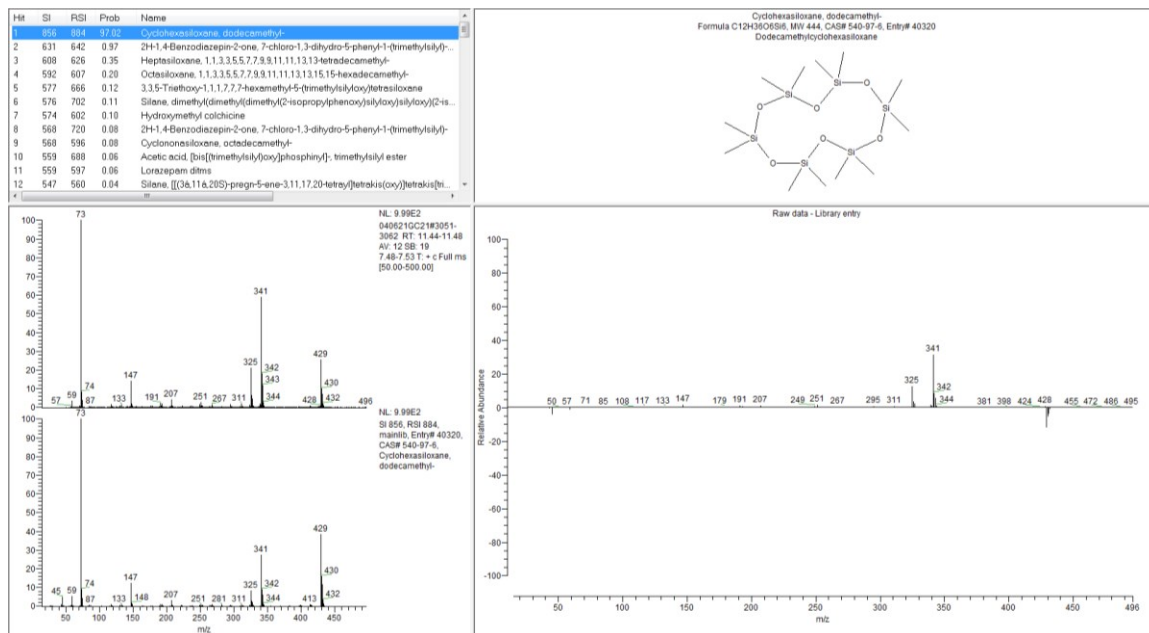


Figure B.13. Identification and Probability of Cyclohexasiloxane, dodecamethyl-

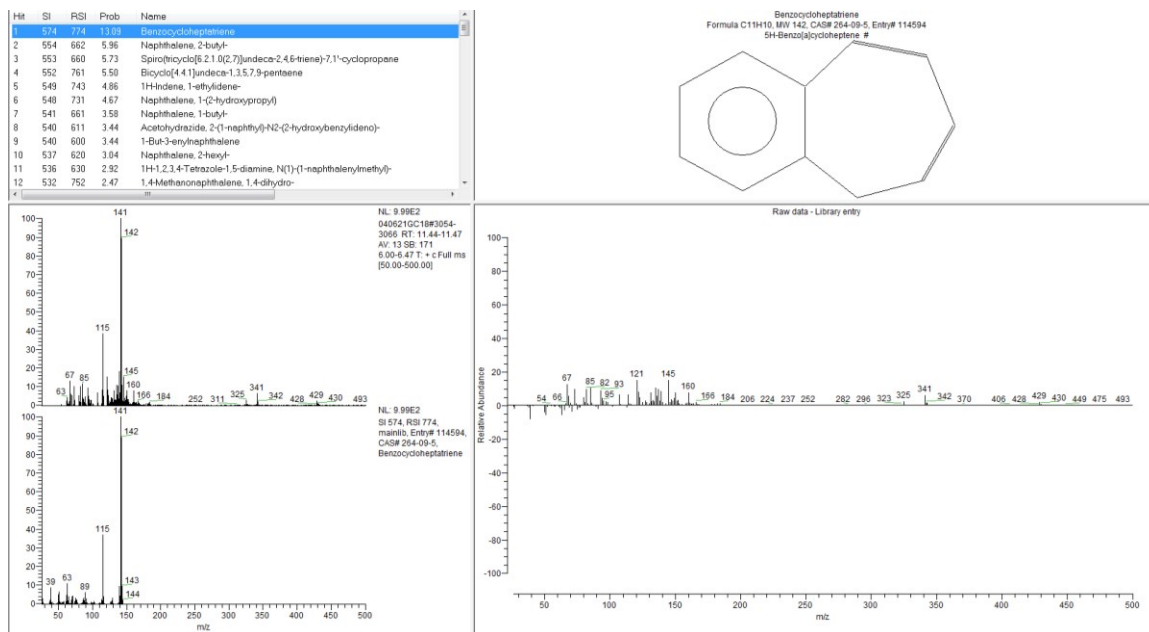


Figure B.14. Identification and Probability of Benzocycloheptatriene

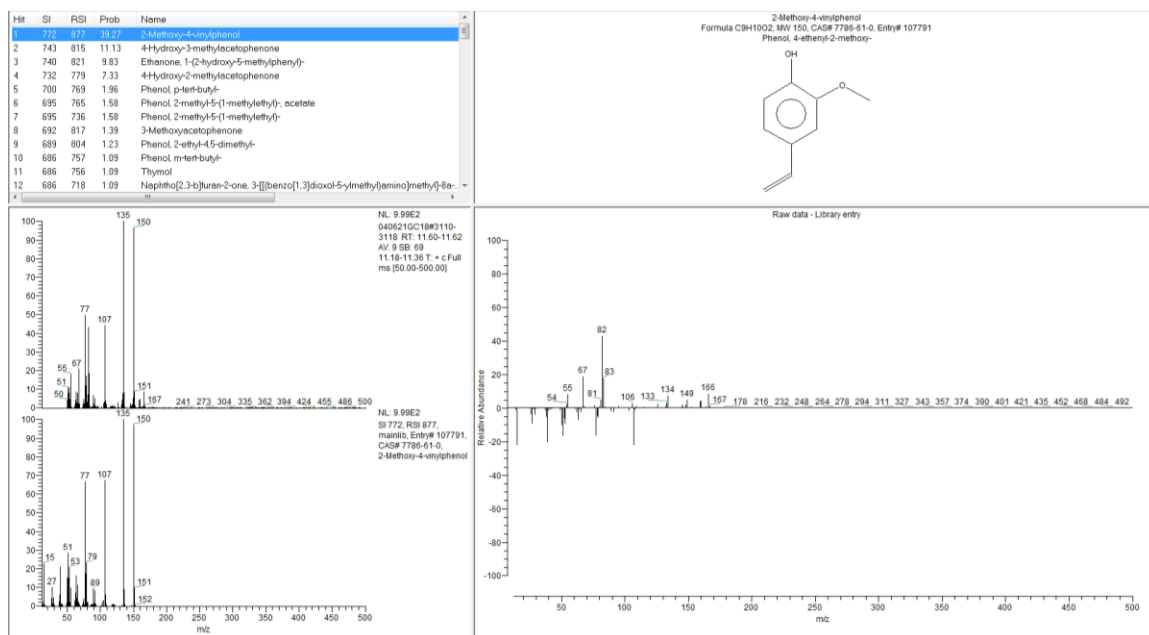


Figure B.15. Identification and Probability of 2-Methoxy-4-vinylphenol

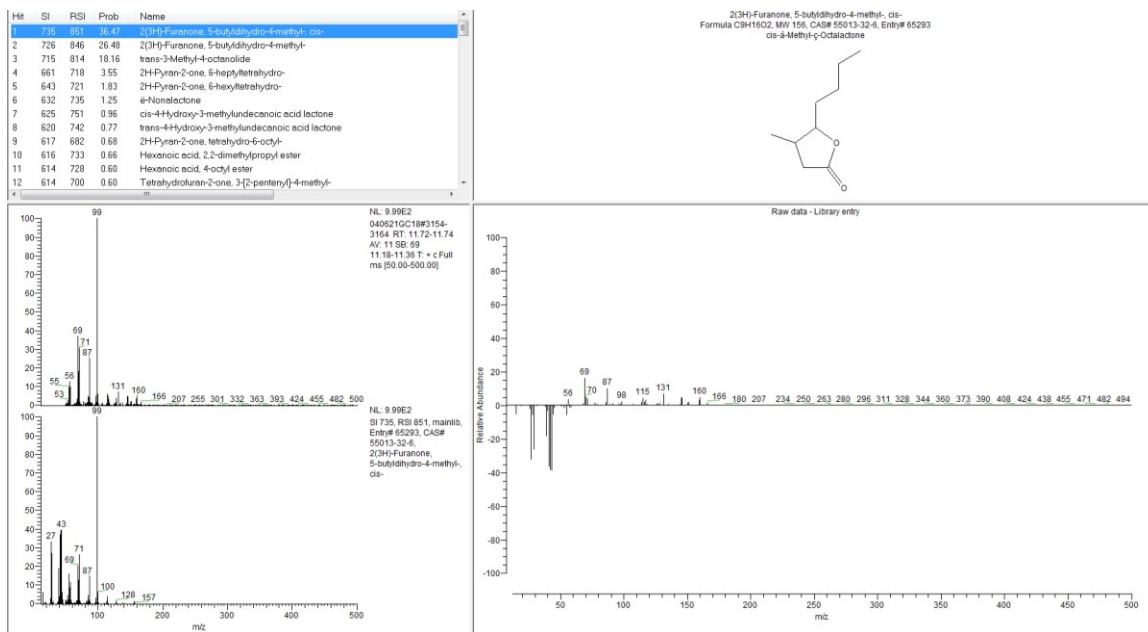


Figure B.16. Identification and Probability of 2(3H)-Furanone, 5-butylidihydro-4-methyl, cis-

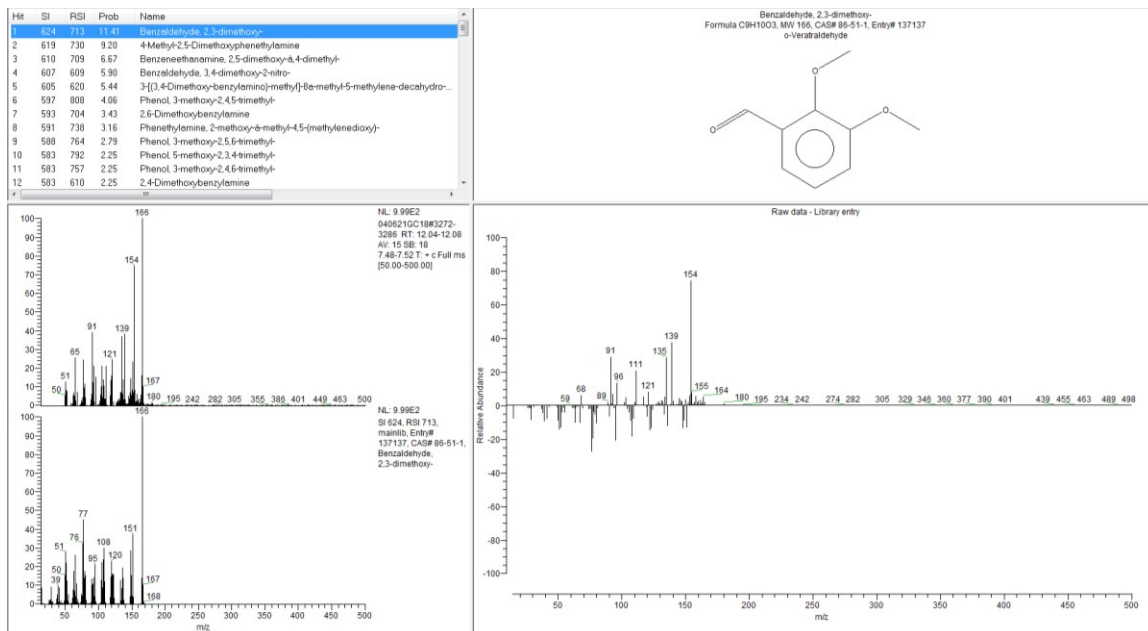


Figure B.17. Identification and Probability of Benzaldehyde, 2,3-dimethoxy-

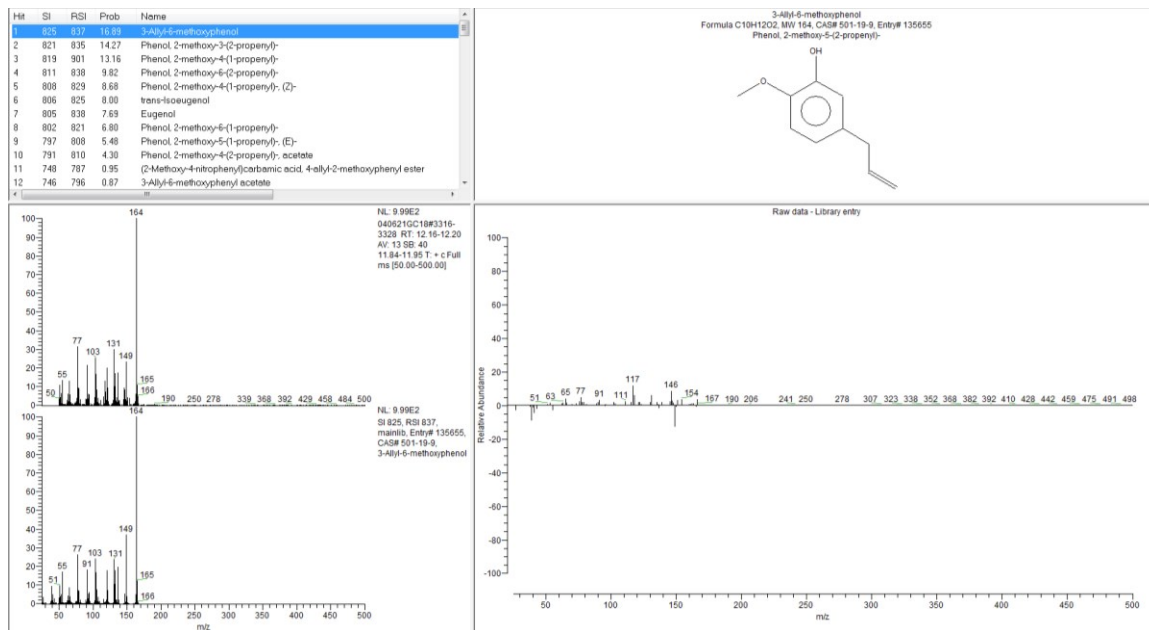


Figure B.18. Identification and Probability of 3-Allyl-6-methoxyphenol

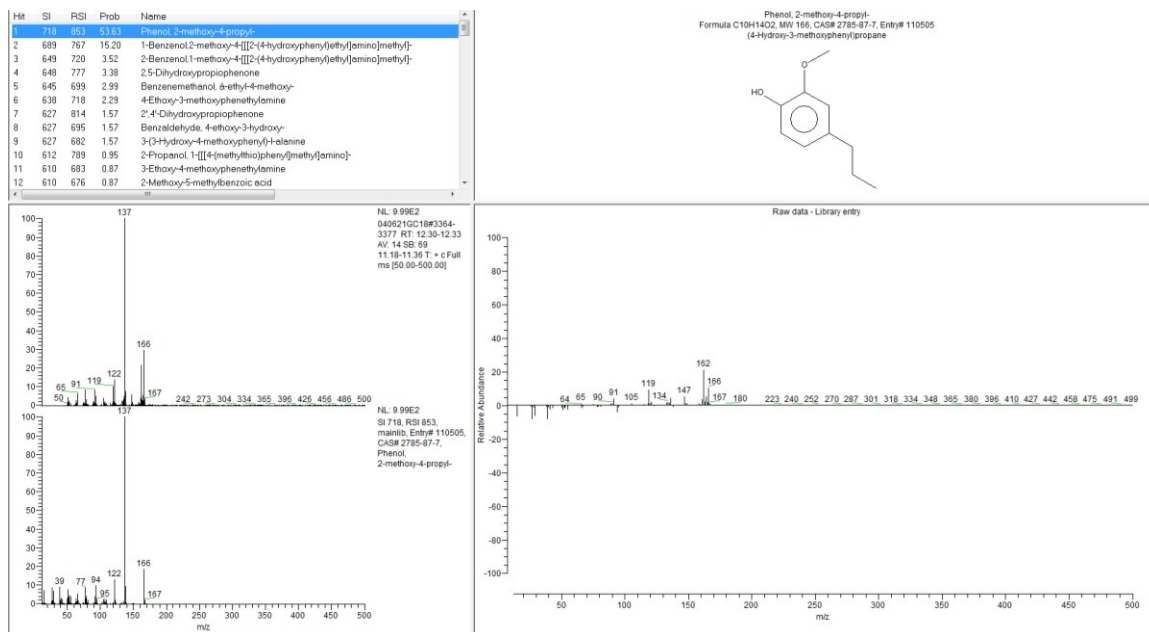


Figure B.19. Identification and Probability of Phenol, 2-methoxy-4-propyl

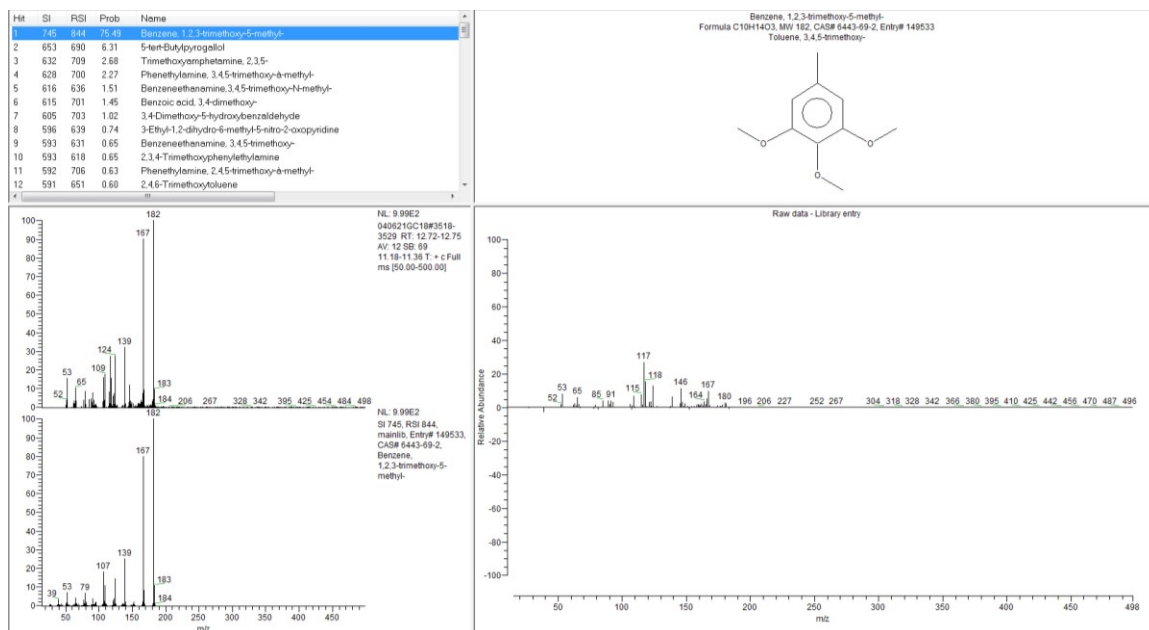


Figure B.20. Identification and Probability of Benzene, 1,2,3-trimethoxy-5-methyl-

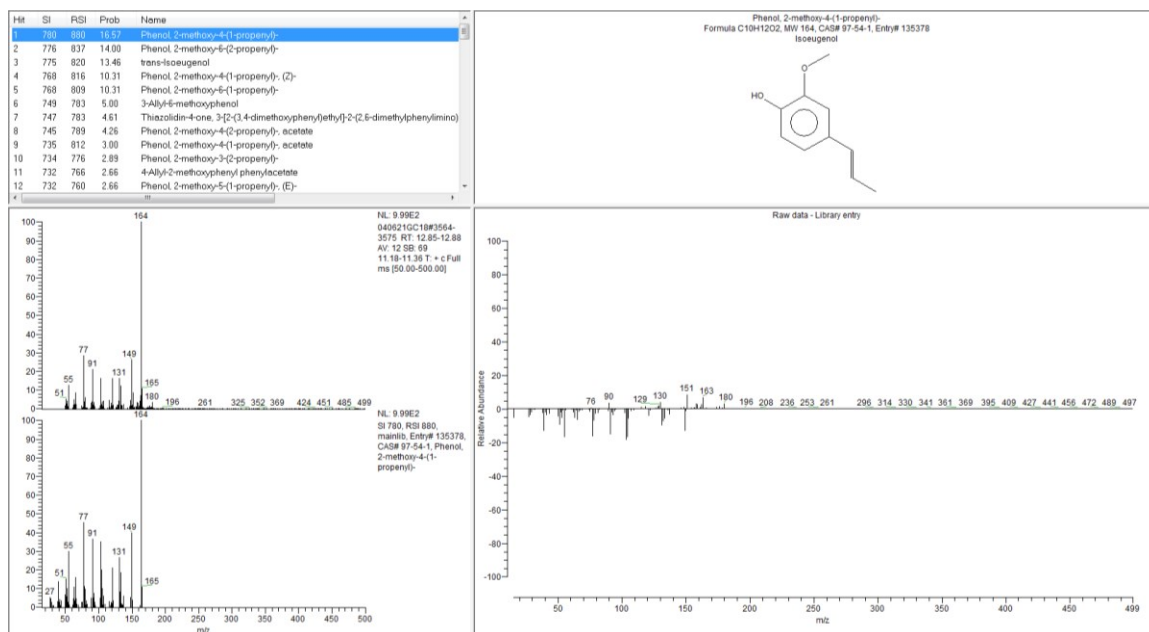


Figure B.21. Identification and Probability of Phenol, 2-methoxy-4-(1-propenyl)- at 12.85 Minutes

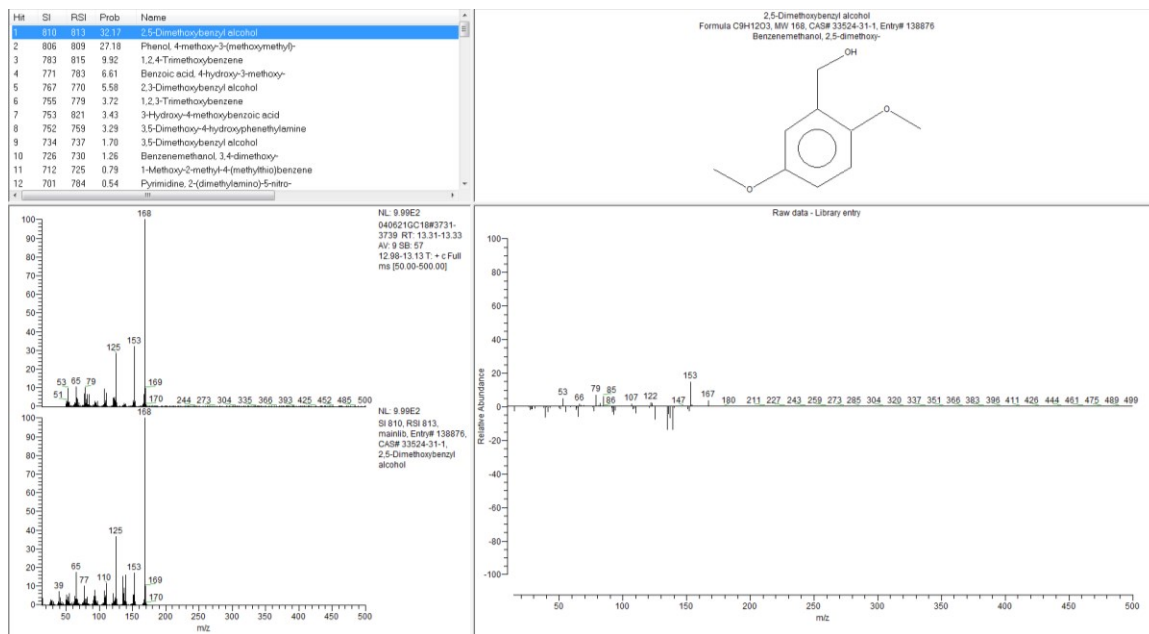


Figure B.22. Identification and Probability of 2,5-Dimethoxybenzyl alcohol

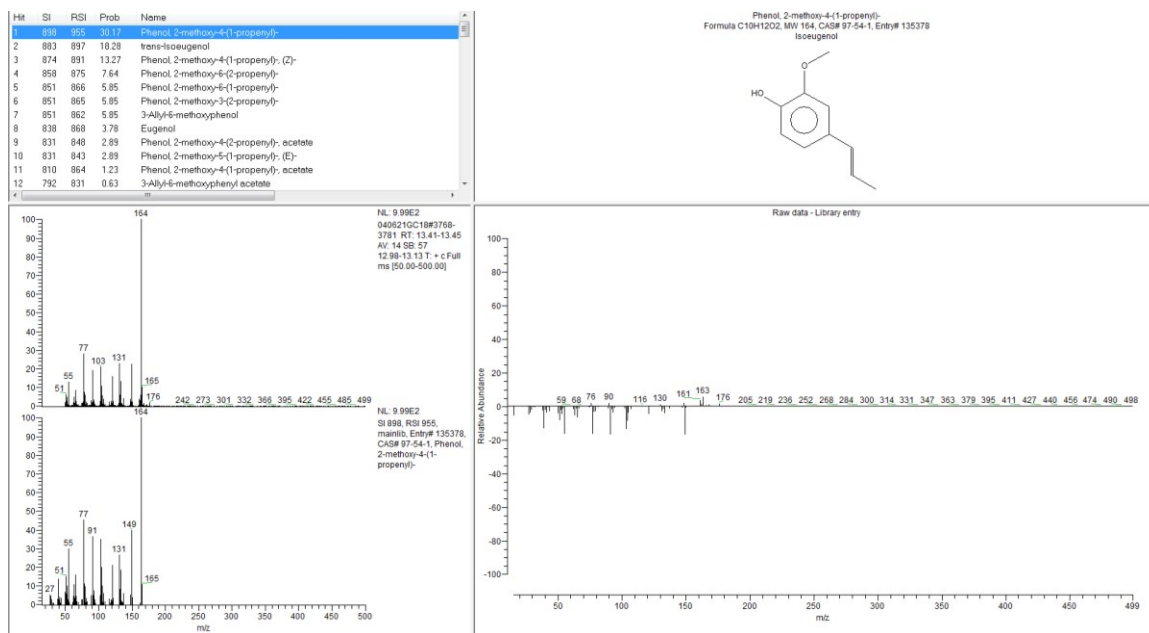


Figure B.23. Identification and Probability of Phenol, 2-methoxy-4-(1-propenyl)- at 13.43 Minutes

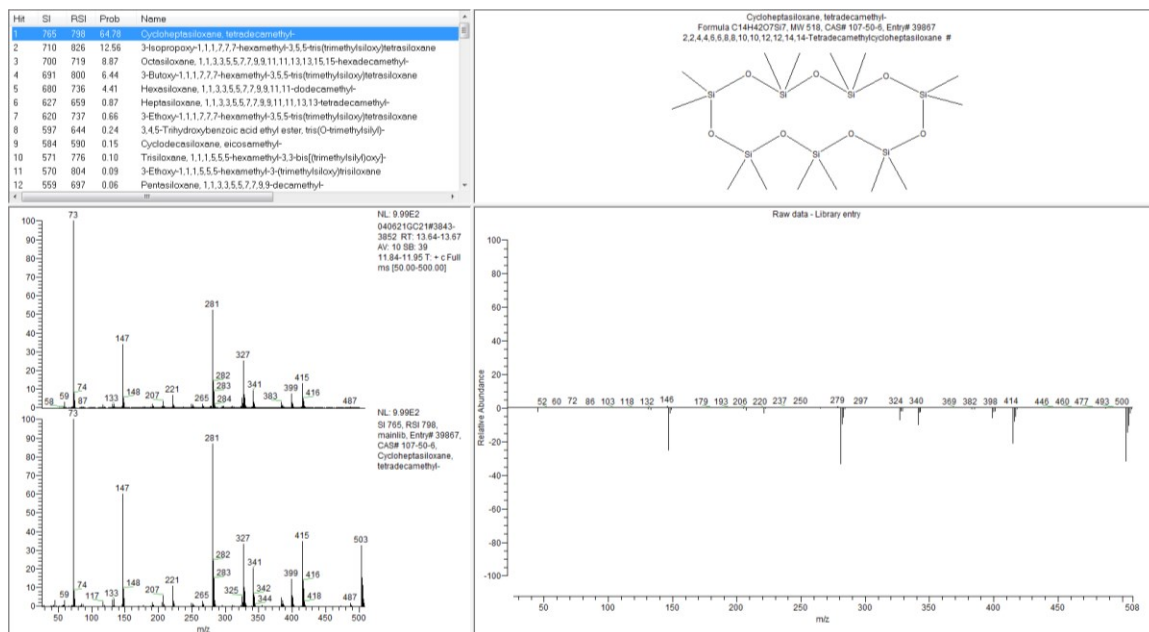


Figure B.24. Identification and Probability of Cycloheptasiloxane, tetradecamethyl-

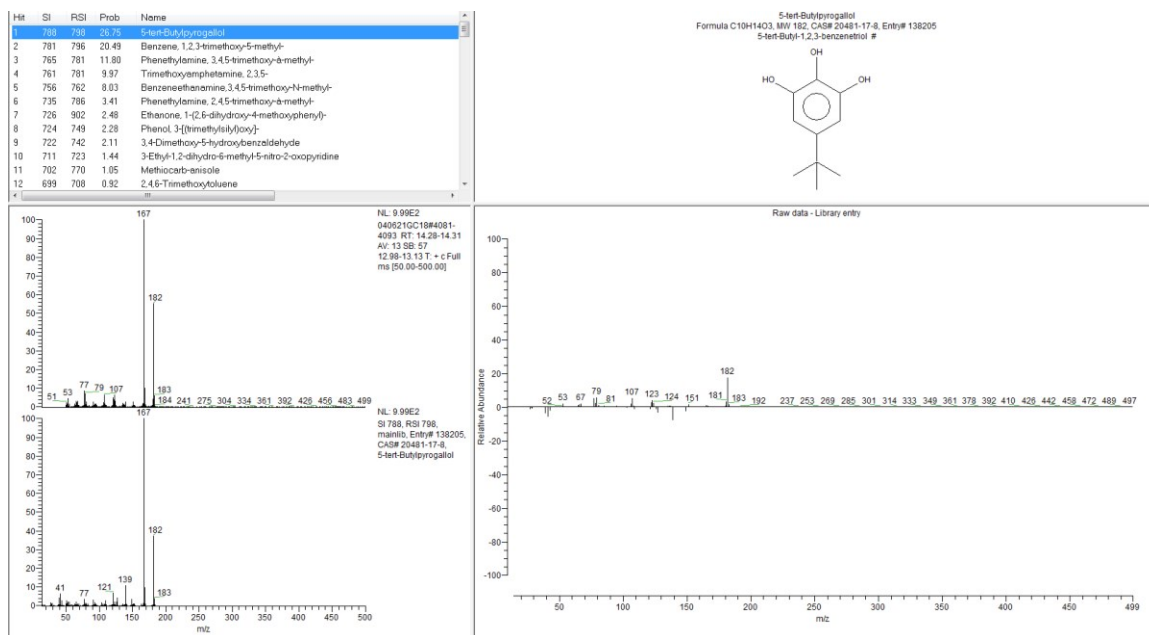


Figure B.25. Identification and Probability of 5-tert-Butylpyrogallol

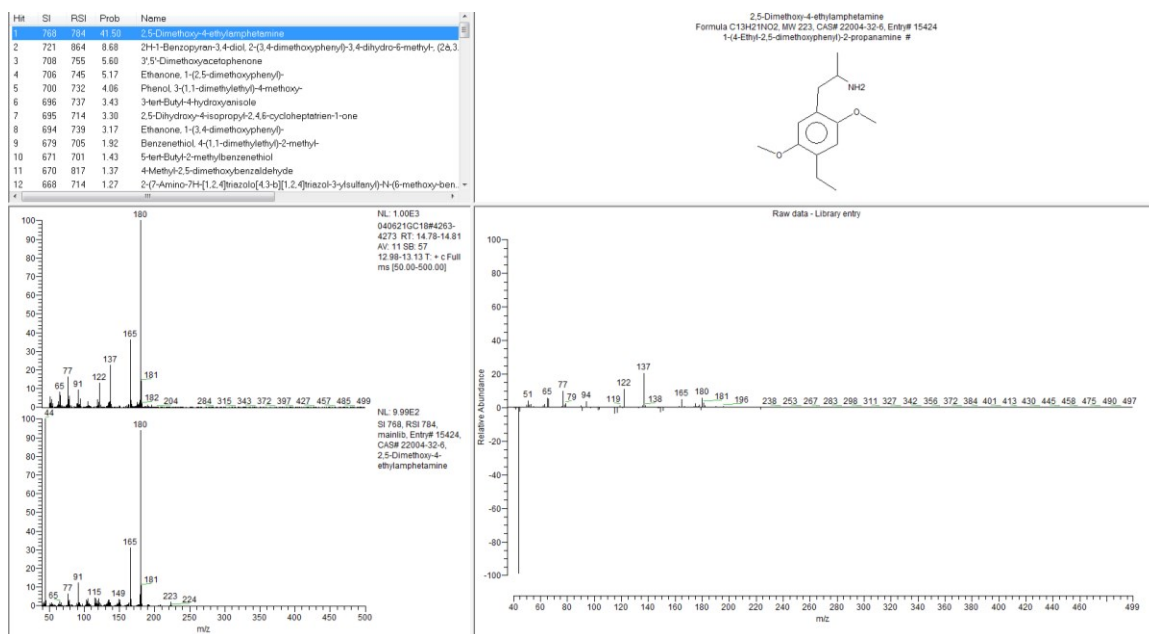


Figure B.26. Identification and Probability of 2,5-Dimethoxybenzyl alcohol

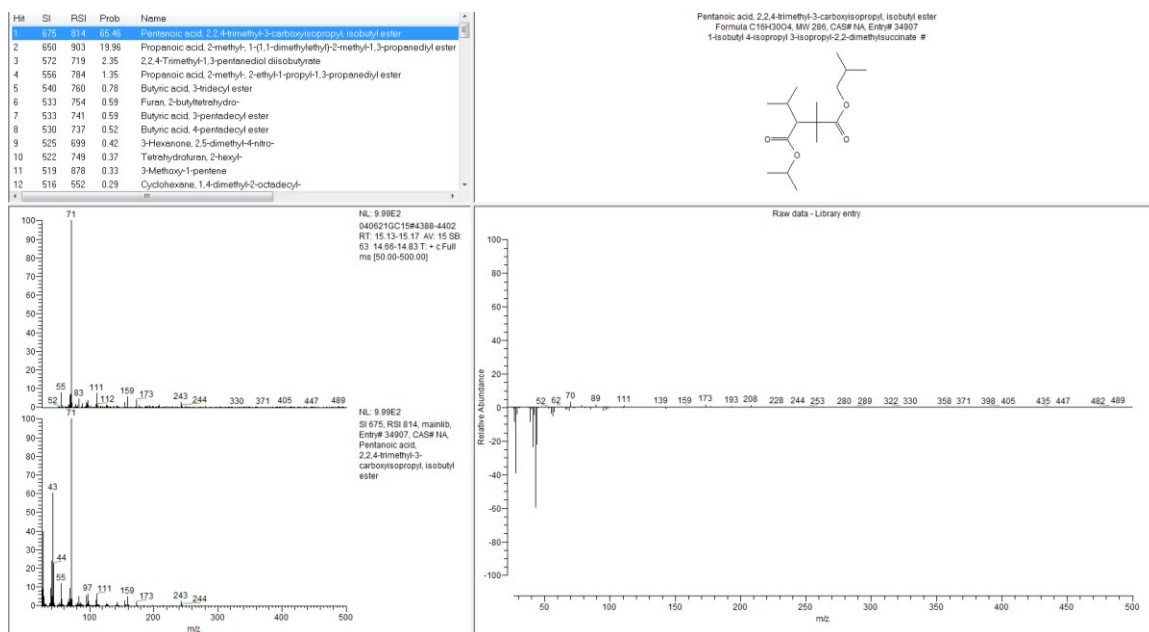


Figure B.27. Identification and Probability of Pentanoic acid, 2,2,4-trimethyl-3-carboxyisopropyl ester

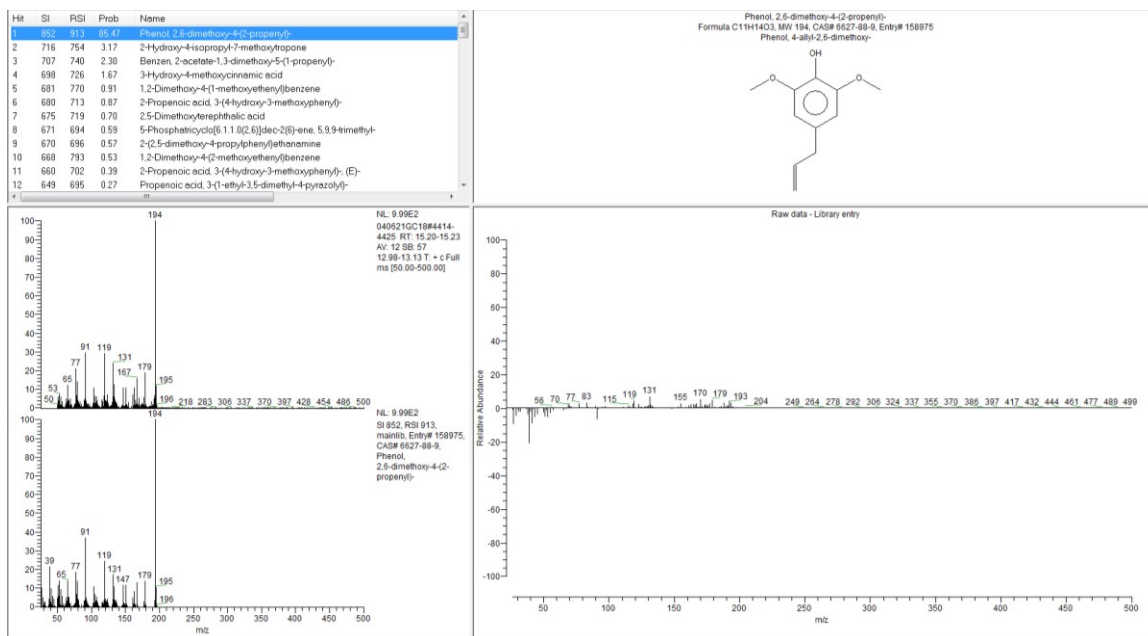


Figure B.28. Identification and Probability of Phenol, 2,6-dimethoxy-4-(2-propenyl)- at 15.20 Minutes

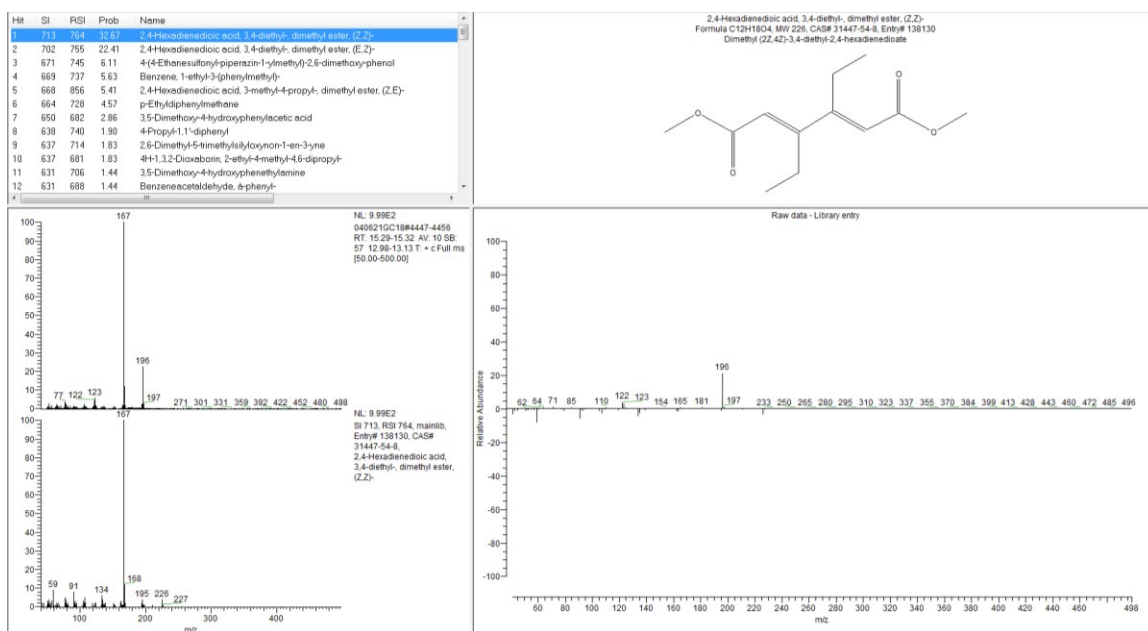


Figure B.29. Identification and Probability of 2,4-Hexadienic acid, 3,4-diethyl-, dimethyl ester

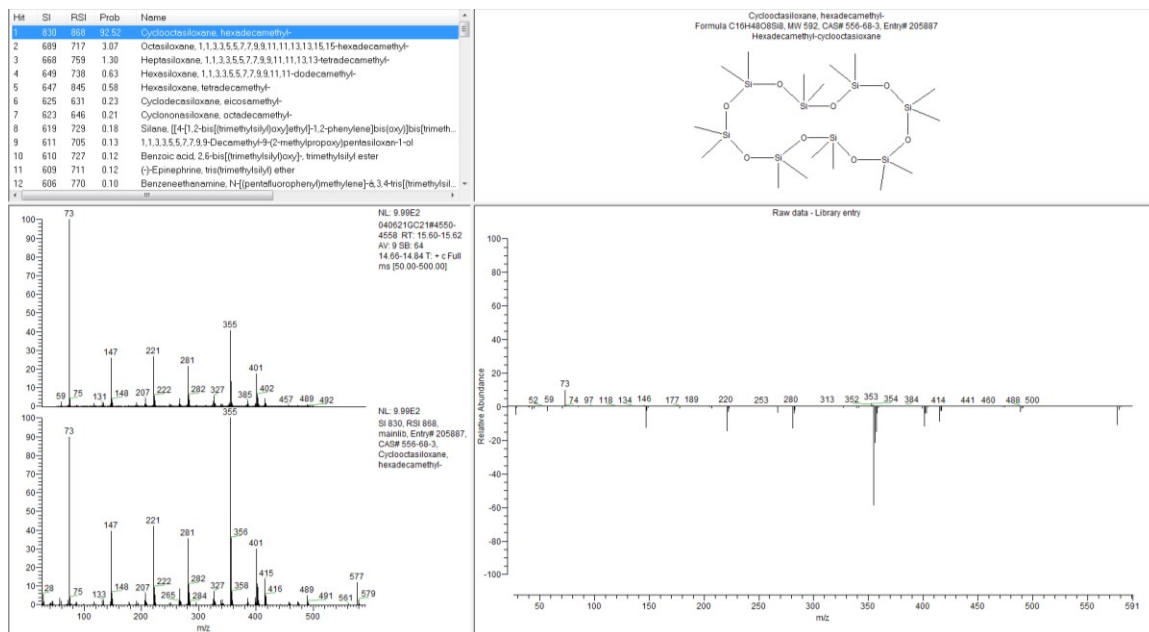


Figure B.30. Identification and Probability of Cyclooctasiloxane, hexadecamethyl-

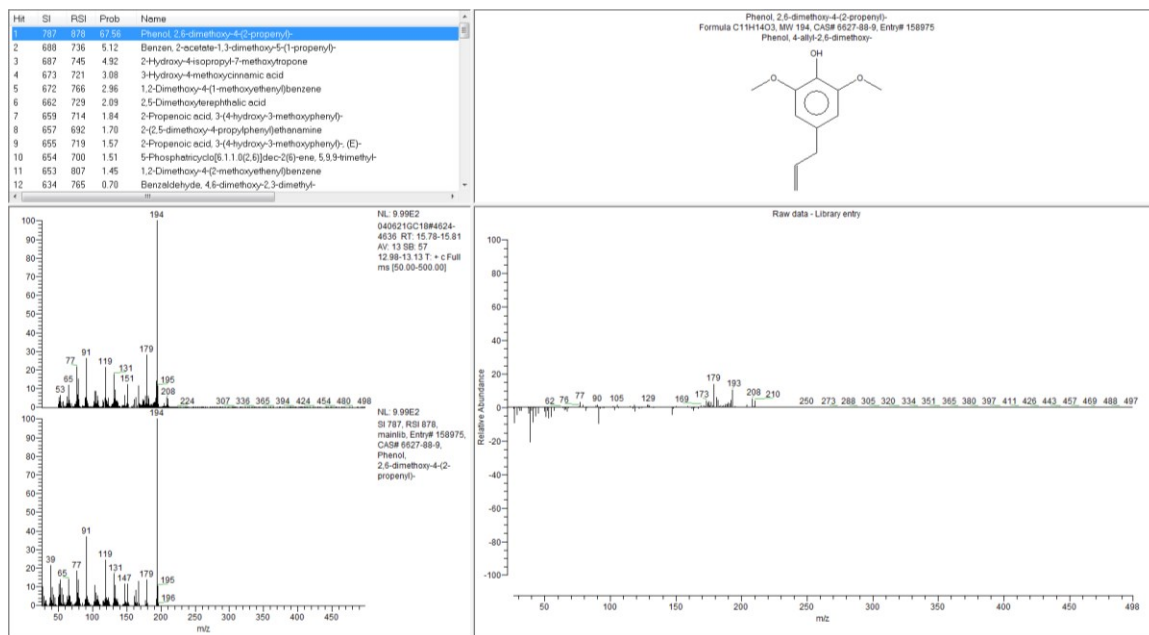


Figure B.31. Identification and Probability of Phenol, 2,6-dimethoxy-4-(2-propenyl)- at 15.80 Minutes

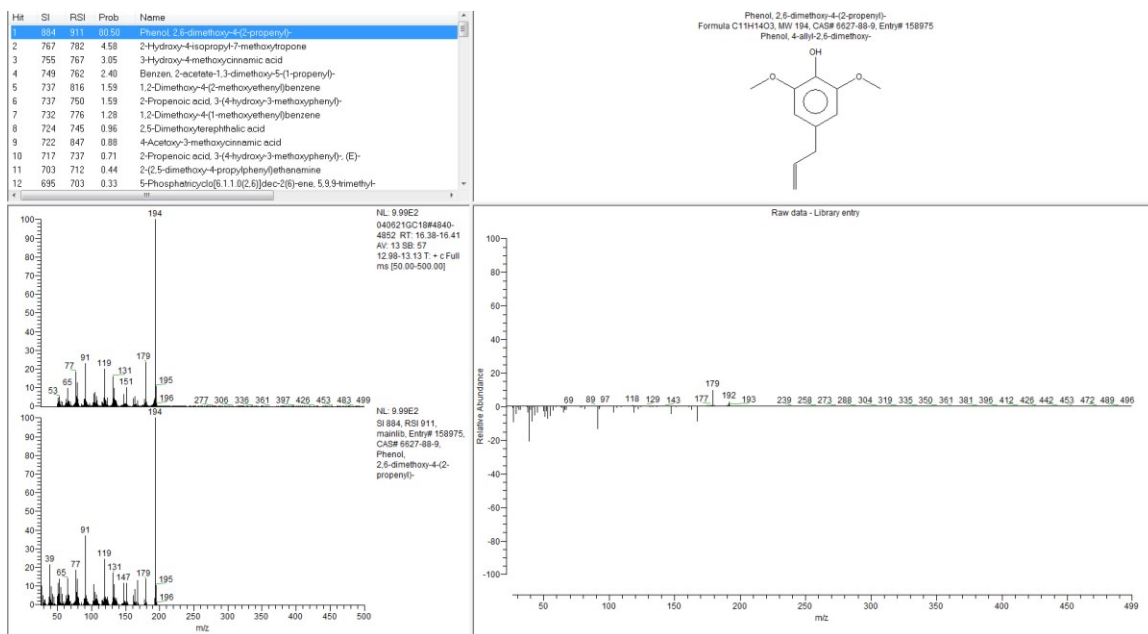


Figure B.32. Identification and Probability of Phenol, 2,6-dimethoxy-4-(2-propenyl)- at 16.39 Minutes

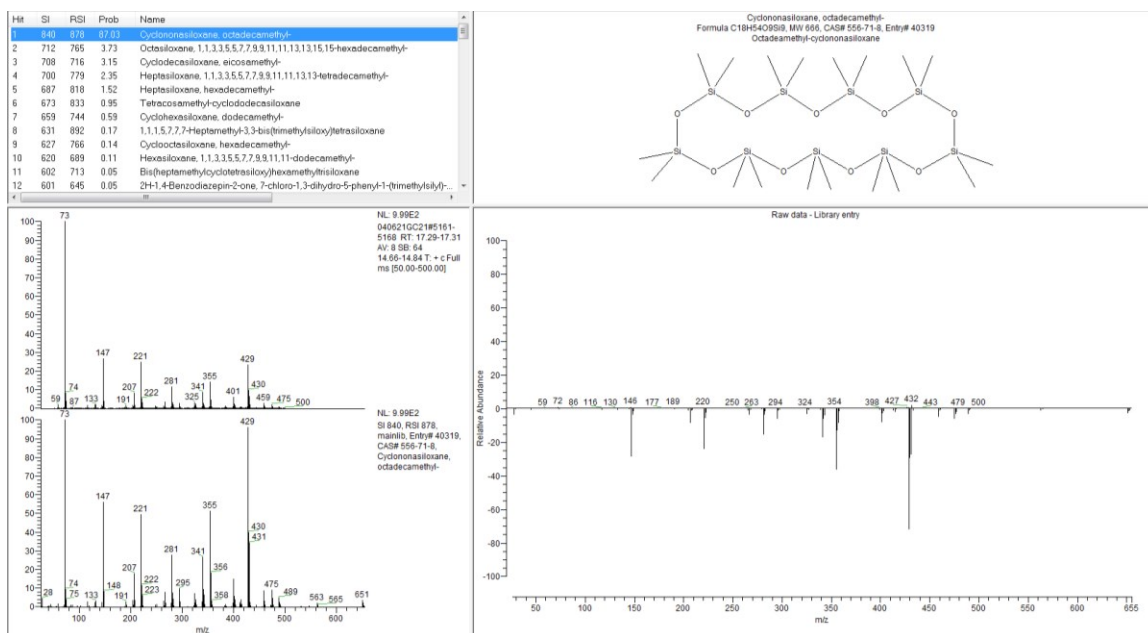


Figure B.33. Identification and Probability of Cyclonasiloxane, octadecamethyl- at 17.30 Minutes

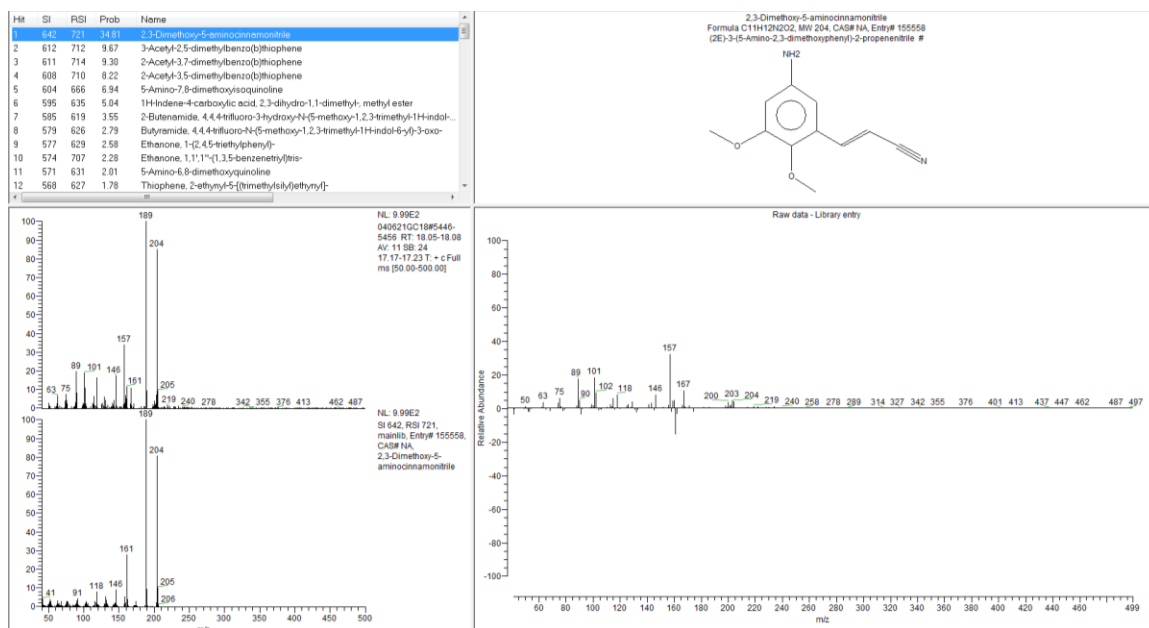


Figure B.34. Identification and Probability of 2,3-Dimethoxy-5-aminocinnamitrile

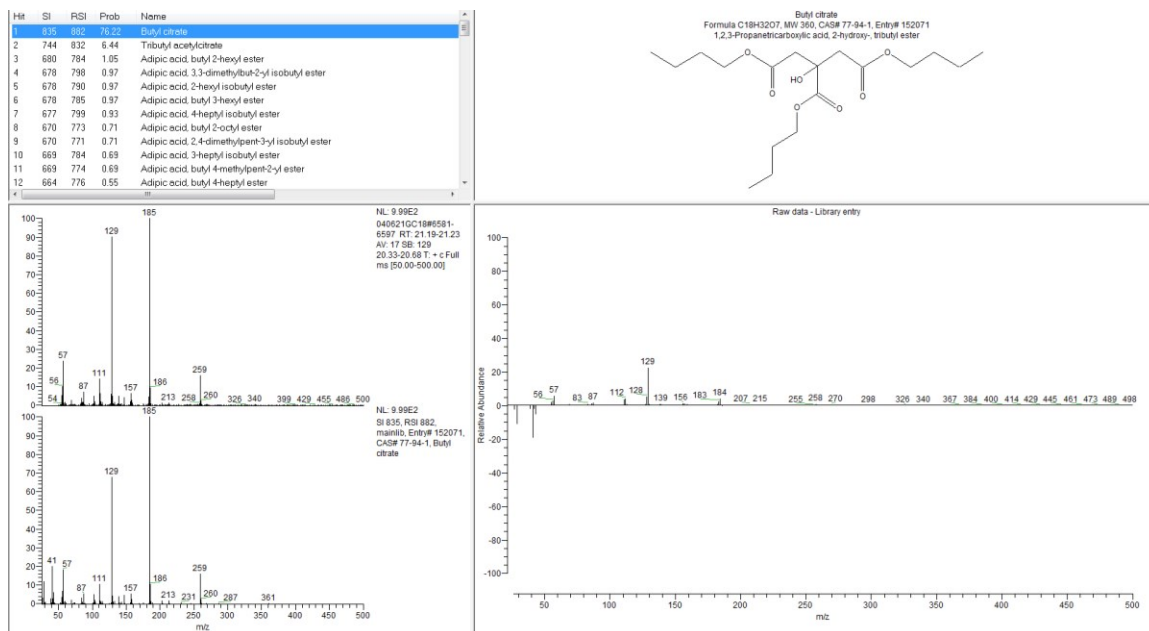


Figure B.35. Identification and Probability of Butyl citrate

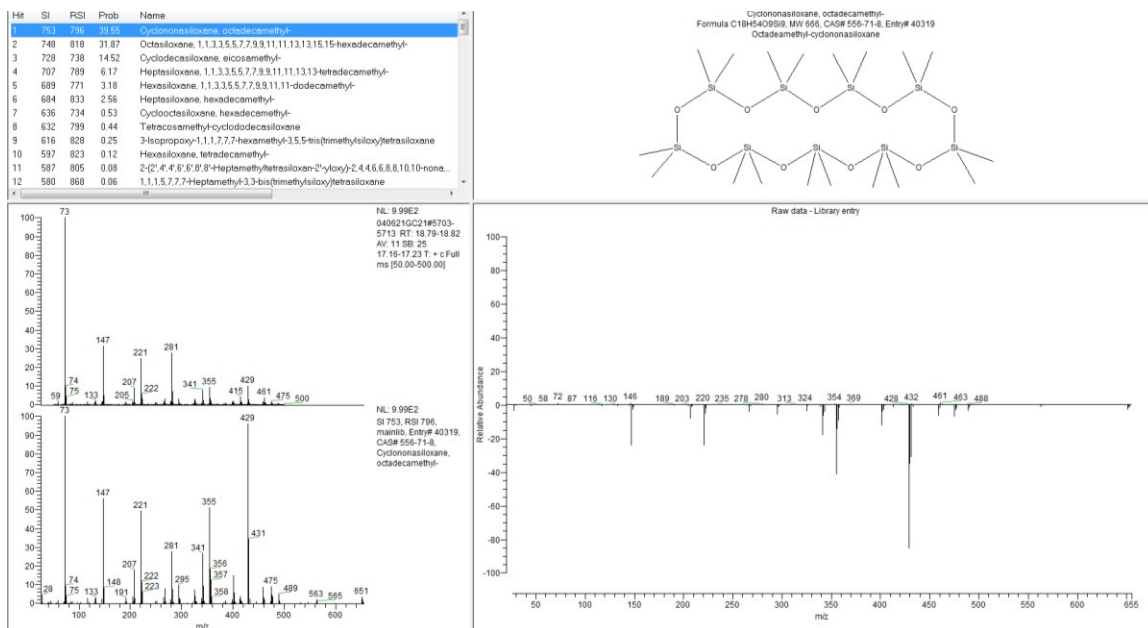


Figure B.36. Identification and Probability of Cyclonasiloxane, octadecamethyl- at 18.81 Minutes

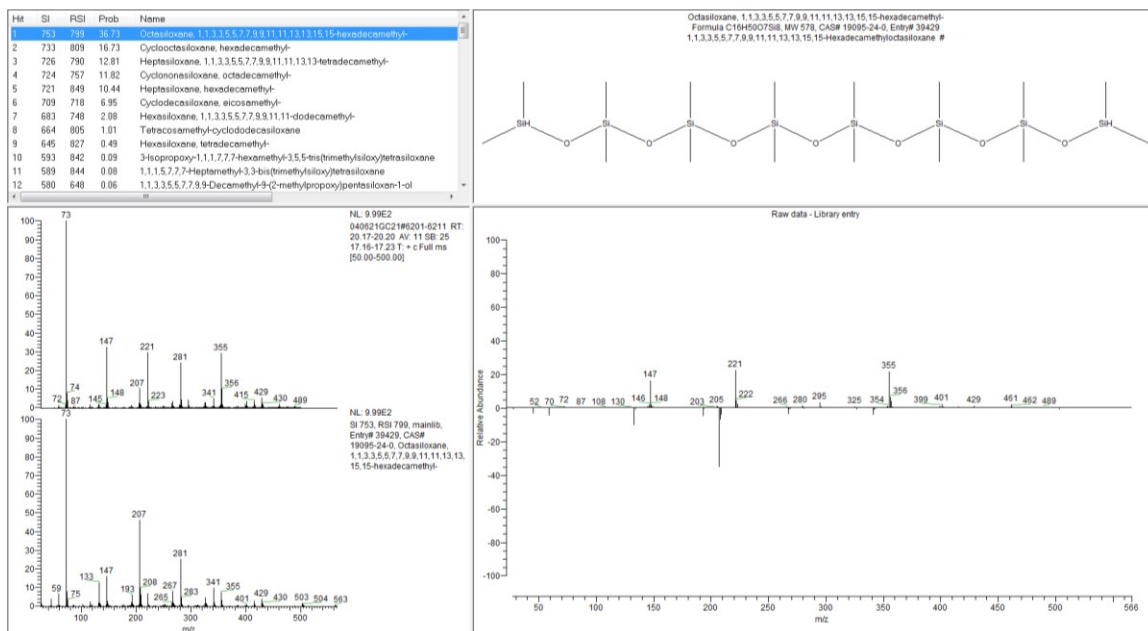


Figure B.37. Identification and Probability of 1H,15H-hexadecamethyloctasiloxane

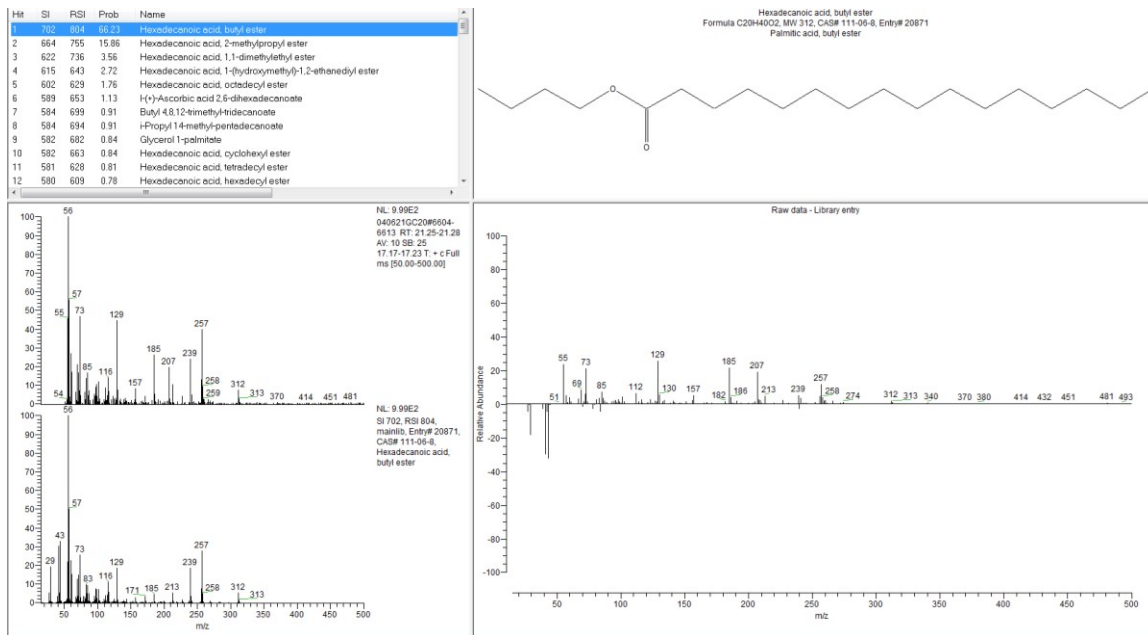


Figure B.38. Identification and Probability of Hexadecanoic acid, butyl ester

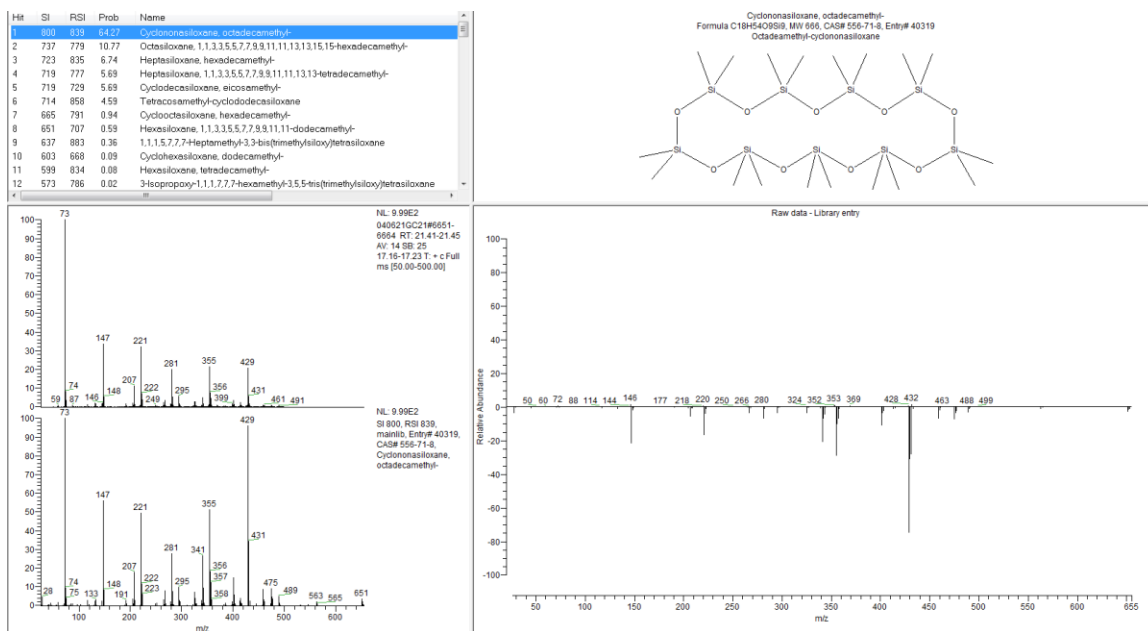


Figure B.39. Identification and Probability of Cyclonasiloxane, octadecamethyl- at 21.43 Minutes

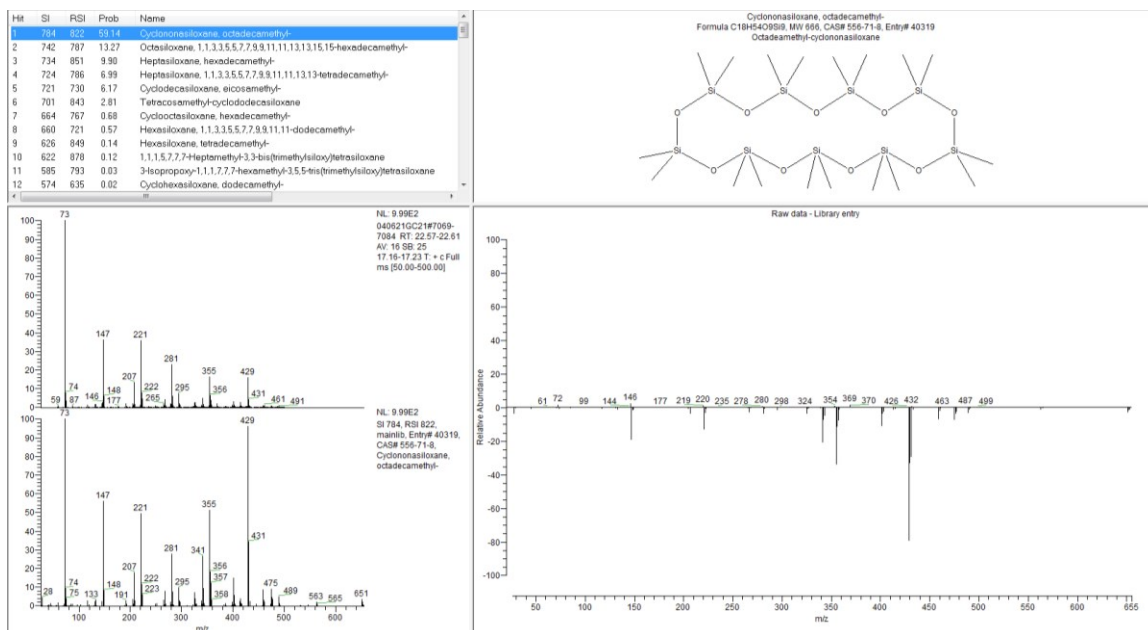


Figure B.40. Identification and Probability of Cyclonasiloxane, octadecamethyl- at 22.59 Minutes

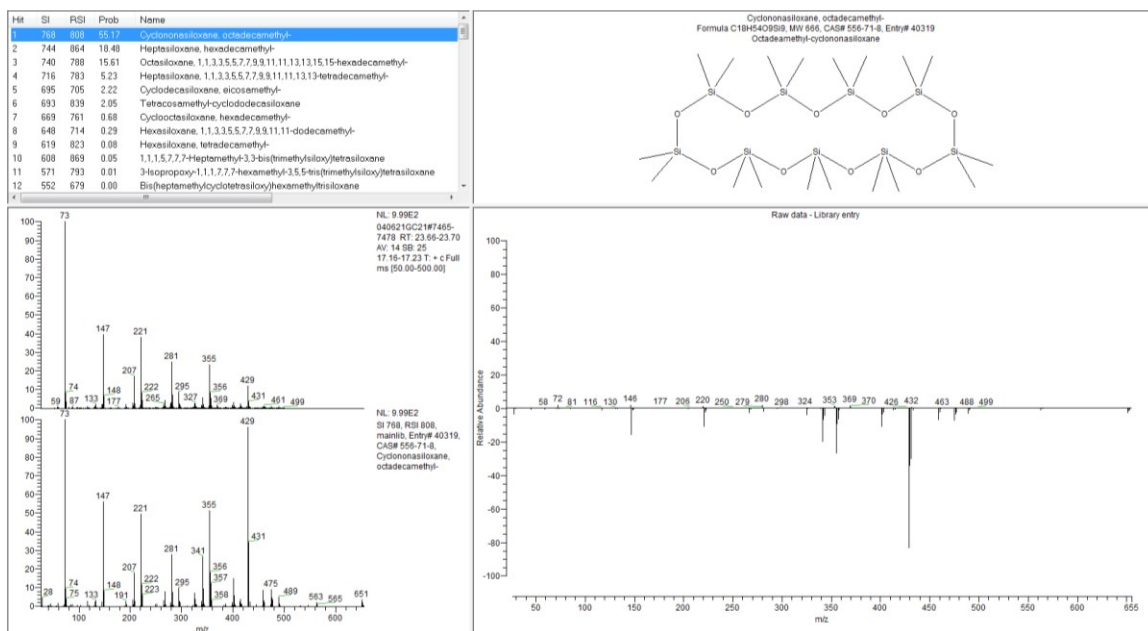


Figure B.41. Identification and Probability of Cyclonasiloxane, octadecamethyl- at 23.68 Minutes

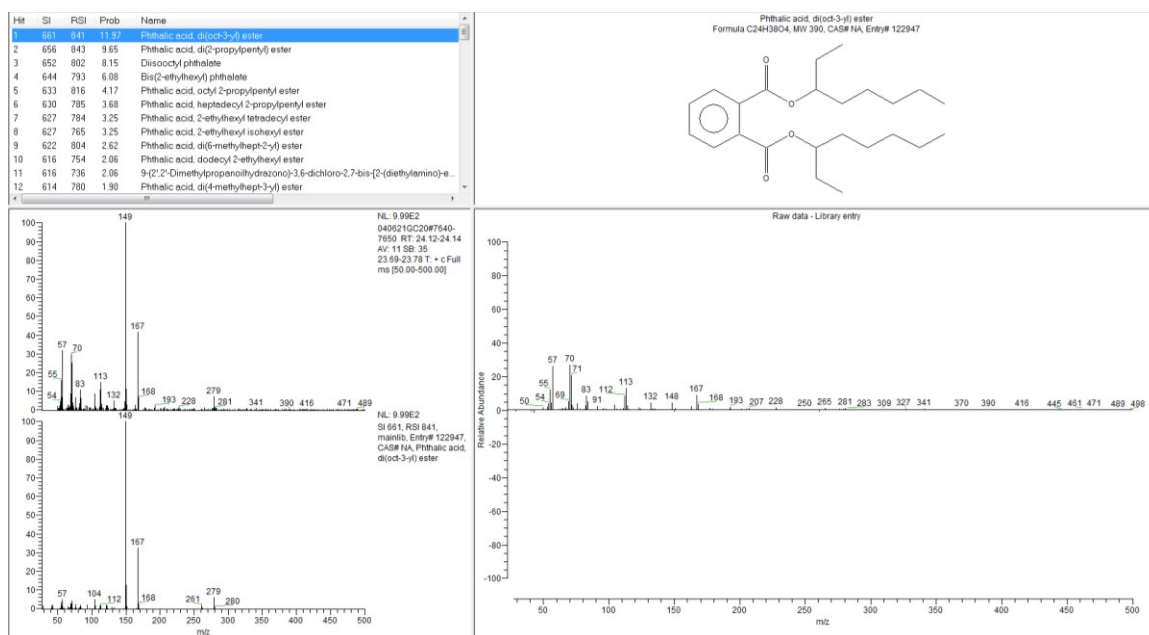


Figure B.42. Identification and Probability of Phthalic acid, di(oct-3-yl) ester

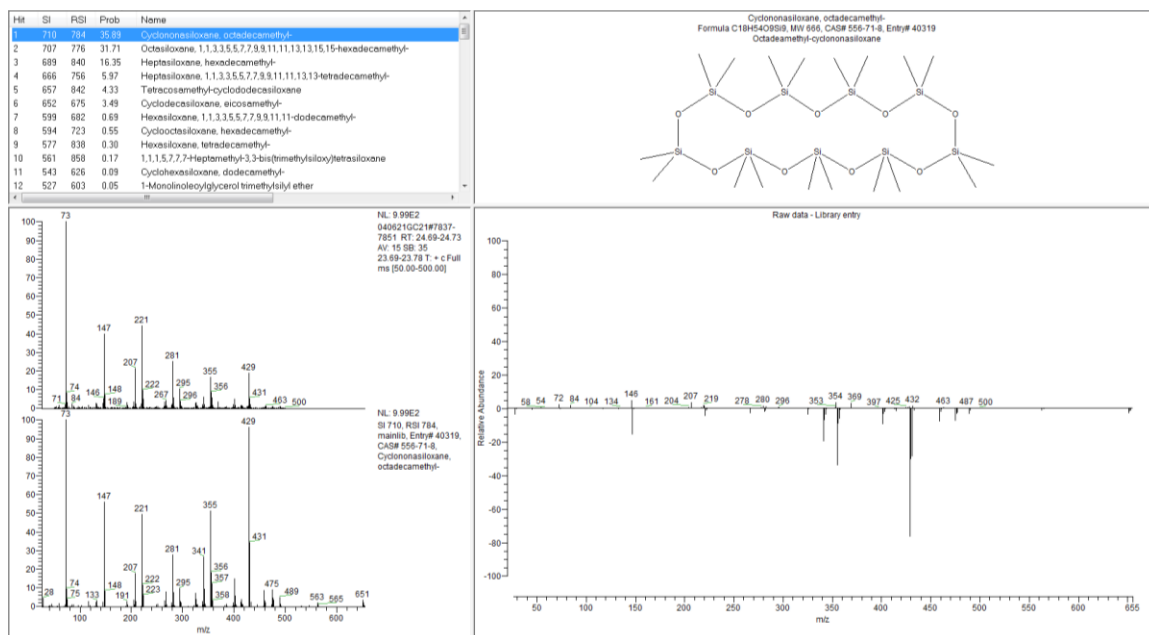


Figure B.43. Identification and Probability of Cyclonasiloxane, octadecamethyl- at 24.72 Minutes

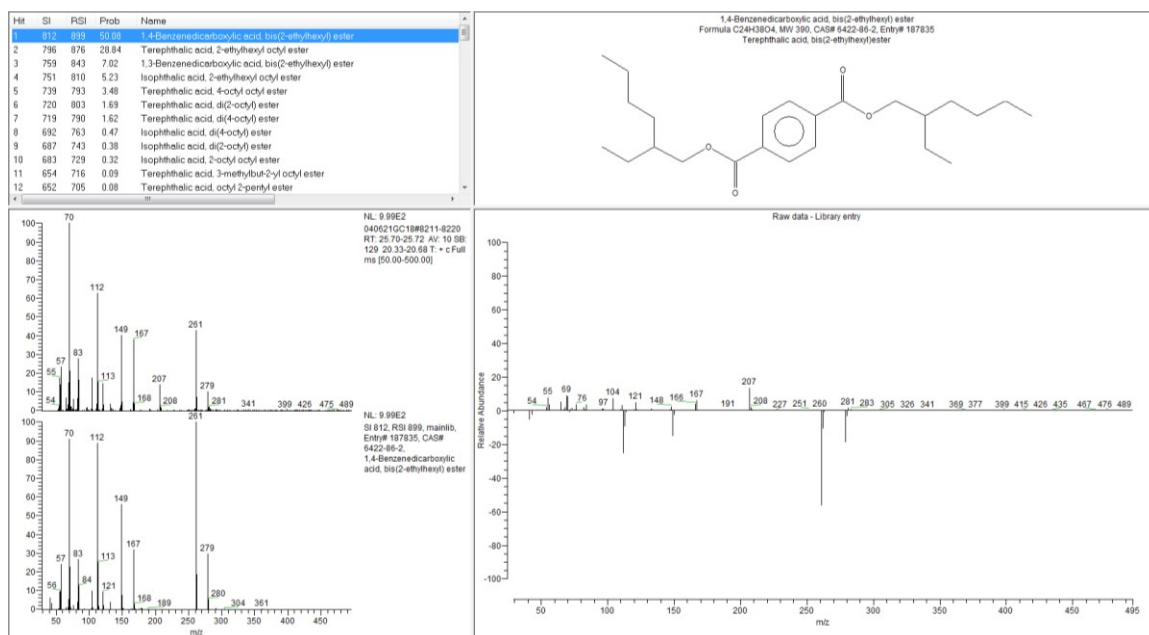


Figure B.44. Identification and Probability of 1,4-Benzenedicarboxylic acid, bis(2-ethylhexyl) ester

BIBLIOGRAPHY

- Blomqvist, P., McNamee, M., Andersson, P., & Lönnermark, A. (2012). Polycyclic Aromatic Hydrocarbons (PAHs) Quantified in Large-Scale Fire Experiments. *Fire Technology*, *48*, 513-528.
- Decamethylcyclopentasiloxane (Compound). Pubchem. <https://pubchem.ncbi.nlm.nih.gov/compound/Decamethylcyclopentasiloxane#section=Use-Classification> (Accessed April 15th, 2021).
- Fent, K. W., Eisenberg, J., Snawder, J., Sammons, D., Pleil, J. D., Stiegel, M. A., . . . Dalton, J. (2014). Systemic exposure to PAHs and benzene in firefighters suppressing controlled structure fires. *Ann Occup Hyg*, *58*(7), 830-845. doi:10.1093/annhyg/meu036
- Parker, J.K., Lignou, S., Shankland, K., Kurwie, P., Griffiths, H.D., Baines, D.A., (2018). Development of a Zeolite Filter for Removing Polycyclic Aromatic Hydrocarbons (PAHs) from Smoke and Smoked Ingredients while Retaining the Smoky Flavor. *Journal of Agricultural and Food Chemistry*, *66*, 2449–2458.. doi:10.1021/acs.jafc.6b05399
- Hu, B., Gao, Z., Wang, H., Wang, J., & Cheng, M. (2020). Computational insights into the sorption mechanism of polycyclic aromatic hydrocarbons by carbon nanotube through density functional theory calculation and molecular dynamics simulation. *Computational Materials Science*, *179*, 109677. doi:<https://doi.org/10.1016/j.commatsci.2020.109677>
- Jeong, K. S., Zhou, J., Griffin, S. C., Jacobs, E. T., Dearmon-Moore, D., Zhai, J., . . . Burgess, J. L. (2018). MicroRNA Changes in Firefighters. *J Occup Environ Med*, *60*(5), 469-474. doi:10.1097/JOM.0000000000001307
- Keir, J. L. A., Akhtar, U. S., Matschke, D. M. J., Kirkham, T. L., Chan, H. M., Ayotte, P., . . . Blais, J. M. (2017). Elevated Exposures to Polycyclic Aromatic Hydrocarbons and Other Organic Mutagens in Ottawa Firefighters Participating in Emergency, On-Shift Fire Suppression. *Environ Sci Technol*, *51*(21), 12745-12755. doi:10.1021/acs.est.7b02850
- Lao, J. Y., Wang, S. Q., Chen, Y. Q., Bao, L. J., Lam, P. K. S., & Zeng, E. Y. (2020). Dermal exposure to particle-bound polycyclic aromatic hydrocarbons from barbecue fume as impacted by physicochemical conditions. *Environ Pollut*, *260*, 114080. doi:10.1016/j.envpol.2020.114080

- Mayer, A. C., Fent, K. W., Bertke, S., Horn, G. P., Smith, D. L., Kerber, S., & La Guardia, M. J. (2019). Firefighter hood contamination: Efficiency of laundering to remove PAHs and FRs. *J Occup Environ Hyg*, *16*(2), 129-140. doi:10.1080/15459624.2018.1540877
- Nazare, S., Flynn, S., Davis, R., & Chin, J. (2014). Protective Performance of Environmentally Stressed Fabrics Containing Melamine Fiber Blends.(Report). *Fire Technology*, *50*(5), 1301.
- Other Carcinogenic Polycyclic Aromatic Hydrocarbons. (2017, March 03). Retrieved September 01, 2020, from <https://www.epa.gov/risk/other-carcinogenic-polycyclic-aromatic-hydrocarbons>
- Polycyclic Aromatic Hydrocarbons (PAHs): Your Environment, Your Health | National Library of Medicine. (2017, May 31). Retrieved August 29, 2020, from <https://toxtown.nlm.nih.gov/chemicals-and-contaminants/polycyclic-aromatic-hydrocarbons-pahs>
- Schneider, M., Stracke, F., Hansen, S., Schaefer, U. (2009). Nanoparticles and their interactions with the dermal barrier. *Dermato Endocrinology*, *1*(4), 197-206.
- Tributyl Citrate. Pubchem. <https://pubchem.ncbi.nlm.nih.gov/compound/Tributyl-citrate#section=GHS-Classification> (accessed April 15th, 2021).
- Yang, K., Zhu, L., & Xing, B. (2006). Adsorption of polycyclic aromatic hydrocarbons by carbon nanomaterials. *Environ Sci Technol*, *40*(6), 1855-1861. doi:10.1021/es052208w
- J. Topinka, L.R. Schwarz, F. Kiefer, F.J. Wiebel, O. Gajdoš, P. Vidová, L. Dobiáš, M. Fried, R.J. Šrám, T. Wolff, DNA adduct formation in mammalian cell cultures by polycyclic aromatic hydrocarbons (PAH) and nitro-PAH in coke oven emission extract, *Mutation Research/Genetic Toxicology and Environmental Mutagenesis*, Volume 419, Issues 1–3, 1998, Pages 91-105, ISSN 1383-5718, [https://doi.org/10.1016/S1383-5718\(98\)00127-2](https://doi.org/10.1016/S1383-5718(98)00127-2).
- Yu H. (2002). Environmental carcinogenic polycyclic aromatic hydrocarbons: photochemistry and phototoxicity. *Journal of environmental science and health. Part C, Environmental carcinogenesis & ecotoxicology reviews*, *20*(2), 149–183. <https://doi.org/10.1081/GNC-120016203>